Baselines of daily quality assurance for proton pencil beam scanning using the Sphinx Compact

Mr. Tanapat Tiajaroen

A Thesis Submitted in Partial Fulfillment of the Requirements
for the Degree of Master of Science in Medical Physics
Department of Radiology
FACULTY OF MEDICINE
Chulalongkorn University
Academic Year 2021

การหาค่าพื้นฐานของการประกันคุณภาพรายวันสำหรับเครื่องโปรตอนประเภทชนิดแสกนนิ่งโดยใช้เครื่องตรวจวัด Sphinx Compact

นายธนภัทร เตียเจริญ

วิทยานิพนธ์นี้เป็นส่วนหนึ่งของการศึกษาตามหลักสูตรปริญญาวิทยาศาสตรมหาบัณฑิต
สาขาวิชาฟิสิกส์การแพทย์ ภาควิชารังสีวิทยา
คณะแพทยศาสตร์ จุฬาลงกรณ์มหาวิทยาลัย
ปีการศึกษา 2564

Thesis Title	Baselines of daily quality assurance for proton pencil beam scanning using the Sphinx Compact
By	Mr. Tanapat Tiajaroen
Field of Study	Medical Physics
Thesis Advisor	Assistant Professor TAWEAP SANGHANGTHUM, Ph.D.

Accepted by the FACULTY OF MEDICINE, Chulalongkorn University in Partial Fulfillment of the Requirement for the Master of Science

.... Dean of the FACULTY OF MEDICINE

(Associate Professor CHANCHAI SITTIPUNT, M.D.)

THESIS COMMITTEE

.... Chairman

(Sornjarod Oonsiri, Ph.D.)

.... Thesis Advisor

(Assistant Professor TAWEAP SANGHANGTHUM, Ph.D.)

.... Examiner

(Mintra Keawsamur, Ph.D.)

.... External Examiner

(Professor Haibo Lin, Ph.D.)

ธนภัทร เตียเจริญ : การหาค่าพื้นฐานของการประกันคุณภาพรายวันสำหรับเครื่องโปรตอนประเภทชนิดแสกนนิ่งโดยใช้เครื่องตรวจวัด Sphinx Compact . (Baselines of daily quality assurance for proton pencil beam scanning using the Sphinx Compact) อ.ที่ปรึกษาหลัก : ผศ. ดร.ทวีป แสงแห่งธรรม

การประกันคุณภาพ (QA) เป็นกระบวนการที่เป็นระบบที่ใช้ในการพิจารณาว่าผลิตภัณฑ์ที่ใช้นั้นตรงตามข้อกำหนดที่ระบุหรือไม่ ในงานทางด้านของรังสีรักษา American Association of Physicists in Medicine (AAPM) ได้มีการเผยแพร่ AAPM TG-224 ซึ่งประกอบไปด้วยขั้นตอนที่จำเป็นทั้งหมดเพื่อให้มั่นใจได้ว่าเครื่องฉายรังสีด้วยอนุภาคโปรตอนสามารถที่จะรักษาผู้ป่วยตามที่ได้รับมอบหมายได้ โรงพยาบาลจุฬาลงกรณ์ (KCMH) เปิดศูนย์การรักษาด้วยอนุภาคโปรตอนแห่งแรกในประเทศไทย และไม่มีข้อมูลของการประกันคุณภาพรายวัน การศึกษานี้มีวัตถุประสงค์เพื่อจะสร้างแผนภูมิควบคุมสำหรับค่าพื้นฐานของการประกันคุณภาพรายวันที่จะใช้สำหรับเครื่องฉายรังสีด้วยอนุภาคโปรตอนประเภทชนิดแสกนนิ่งโดยใช้เครื่องตรวจวัด สฟิงซ์ คอมแพค (Sphinx Compact) เนื่องจากแผนภูมิควบคุมสามารถที่จะใช้เพื่อประเมินข้อมูลการประกันคุณภาพรายวันเพื่อตรวจสอบว่าการวัดแต่ละรายการจำเป็นต้องดำเนินการหรือไม่

สฟิงซ์ คอมแพค (Sphinx Compact) ถูกใช้เพื่อทำการประกันคุณภาพรายวันเครื่องฉายรังสีด้วยอนุภาคโปรตอนเป็นเวลา 93 วัน และวิเคราะห์ผลโดยซอฟต์แวร์ myQA ตามคำแนะนำ AAPM TG-224 ค่าพื้นฐานที่ได้จากแผนภูมิควบคุมถูกแบ่งออกเป็น 5 หัวข้อ: 1) การตรวจสอบความลึกประกอบไปด้วย Proximal and Distal depth, Distal falloff, และ Peak width ที่พลังงาน 100 MeV (เมกะ อิเล็กตรอน โวลต์), 150 MeV และ 200 MeV, 2) ลักษณะเฉพาะของสพอท (spot) ประกอบด้วยตำแหน่ง, ความกว้าง (sigma), ความเบ้, และความเข้มของสพอท ที่พลังงาน 70 MeV, 100 MeV, 125 MeV, 150 MeV, 175 MeV, และ 200 MeV, 3) x-ray/proton coincidence, 4) Homogeneity, และ 5) ปริมาณรังสี (dose output) ขีดจำกัดการควบคุมบนและล่างของแผนภูมิควบคุมคำนวณจากข้อมูลที่ต่อเนื่องกัน 50 ข้อมูลในการทดสอบแต่ละหัวข้อ

ผลลัพธ์ของขีดจำกัดการควบคุมทั้งหมดน้อยกว่าขีดจำกัดที่เผยแพร่โดย AAPM TG-224 ขีดจำกัดสูงสุดของ Distal depth, Proximal depth, Distal falloff, และ Peak width คือ ± 0.5 มม. จากพลังงาน 200 MeV สำหรับลักษณะเฉพาะสพอท ขีดจำกัดสูงสุดของตำแหน่ง, ความกว้าง, ความเบ้ ,และความเข้ม คือ ± 1.2 มม., ± 2.9 มม., ± 0.621, ± 1.8 % ตามลำดับ สำหรับ x-ray/proton coincidence พบว่าขีดจำกัดคือ ± 0.4 มม. และ ± 0.2 มม. ในทิศทางด้านแกนเอ็กซ์ (X) และวาย (Y) ตามลำดับ ขีดจำกัดของ Homogeneity และปริมาณรังสี คือ ± 0.7 % และ ± 0.010 นาโนคูลอมบ์ ตามลำดับ

โดยสรุป แผนภูมิควบคุมที่ได้จาก Sphinx Compact สามารถที่จะใช้เพื่อกำหนดค่าพื้นฐานของการทำประกันคุณภาพรายวันสำหรับเครื่องโปรตอนประเภทชนิดแสกนนิ่งที่ศูนย์โปรตอนสมเด็จพระเทพรัตนราชสุดาฯ โรงพยาบาลจุฬาลงกรณ์

สาขาวิชา	ฟิสิกส์การแพทย์	ลายมือชื่อนิสิต	....
ปีการศึกษา	2564	ลายมือชื่อ อ.ที่ปรึกษาหลัก	....

6370016430 : MAJOR MEDICAL PHYSICS
KEYWORD: Baselines, Pencil beam scanning, Sphinx Compact, Quality assurance

Tanapat Tiajaroen : Baselines of daily quality assurance for proton pencil beam scanning using the Sphinx Compact . Advisor: Asst. Prof. TAWEAP SANGHANGTHUM, Ph.D.

Quality assurance (QA) is a systematic process used to determine whether the product meets specified requirements. The American Association of Physicists in Medicine (AAPM) published a comprehensive proton therapy machine QA in TG-224 to provide confidence in use. King Chulalongkorn Memorial Hospital (KCMH) recently operated the first proton therapy center in Thailand, and the data of daily QA are not available or established. This study aims to apply the control chart for establishing the baselines of daily QA for the proton pencil beam scanning system using the Sphinx Compact detector.

The Sphinx Compact was used to perform the proton daily QA test for a total of 93 days and analyzed by myQA software according to the AAPM TG-224 recommendation. The baselines obtained by a control chart were divided into 5 subjects: 1) the depth verification including the distal and proximal depth, distal falloff, and peak width of 100 MeV, 150 MeV, and 200 MeV, 2) spot characteristics including position, sigma, skewness, and intensity of 70 MeV, 100 MeV, 125 MeV, 150 MeV, 175 MeV, and 200 MeV, 3) x-ray/proton coincidence, 4) homogeneity and 5) dose output. The upper and lower control limits (UCL and LCL) of the control chart were calculated from 50 consecutive data in each test.

All the results of control limits were found to be less than the limits recommended by AAPM TG-224. The highest limits of distal depth, distal fall-off, proximal depth, and peak width were ± 0.5 mm in all tasks from 200 MeV. For spot characteristics, the highest limits of spot position, spot sigma, spot skewness, and intensity were ± 1.2 mm, ± 2.9 mm, ± 0.621, and ± 1.8 % respectively. For x-ray/proton coincidence, the limits were found to be ± 0.4 mm and ± 0.2 mm in X and Y directions, respectively. The limits of uniform field homogeneity and dose output consistency were ± 0.7 % and ± 0.010 nC, respectively.

In conclusion, the control charts obtained by Sphinx Compact can be applied to set the baselines of daily QA data for proton pencil beam scanning at Her Royal Highness Princess Maha Chakri Sirindhorn Proton Therapy Center, KCMH.

Field of Study:	Medical Physics	Student's Signature	
Academic Year:	2021	Advisor's Signature	

ACKNOWLEDGEMENTS

First and foremost, I would like to express my sincere gratitude to my advisor, Assistant Professor Tawaep Sanghangthum, Ph.D., and Mintra Keawsamur, Ph.D., for their continuous support of my M.Sc. study and research and invaluable help throughout this thesis.

I express my special thank to the radiation therapy technologist staff for their assistance in conducting the data.

I am thankful to all the lecturers, medical physicists, and staff at the medical physics program, Faculty of Medicine, Chulalongkorn University for their suggestions and teaching knowledge during my M.Sc. study.

I thank my colleagues in medical physics for their academic support and friendly environment for all the fun we had in two years. Completing this work would have been ever more difficult were it not for the support and friendship provided by the team.

Tanapat Tiajaroen

TABLE OF CONTENTS

Page

.... iii

ABSTRACT (THAI) iii

.... iv

ABSTRACT (ENGLISH) iv

ACKNOWLEDGEMENTS v

TABLE OF CONTENTS vi

LIST OF TABLES ix

LIST OF FIGURES xi

LIST OF ABBREVIATIONS x

Chapter 1 1

1.1 Background and rationale 1

1.2 Research objective 4

Chapter 2 5

2.1 Theory 5

2.1.1 Proton interaction mechanisms 5

2.1.2 Proton Bragg peak curve 6

2.1.3 Proton pencil beam scanning 9

2.1.4 Flat-panel detector 10

2.1.5 Ionization chamber detector 11

2.1.6 X bar/moving range control chart 12

2.2 Review of related literature 12

Chapter 3 18

3.1 Research design 18

3.2 Conceptual framework 18

3.3 Research design model 18

3.4 Research question 19

3.5 Research objective 19

3.6 Materials 19

3.6.1 Proton therapy system 19

3.6.2 Sphinx Compact QA device 20

3.6.3 myQA software 22

3.7 Methods 23

3.7.1 Daily QA test of proton pencil beam scanning 23

3.8 Statistical analysis 24

3.9 Data analysis 24

3.10 Outcome 25

3.11 Expected benefits 25

3.12 Limitation 25

3.13 Ethical consideration 25

Chapter 4 26

4.1 Energy characteristics 26

4.2 Spot characteristics 29

4.3 Uniform field homogeneity 40

4.4 Coincidence 40

4.5 Dose output consistency 40

Chapter 5 43

5.1 Energy characteristics 43

5.2 Spot characteristics 44

5.3 X-ray/proton coincidence 48

5.4 myQA control limits setup 49

5.5 Conclusion 53

REFERENCES 54

VITA 57

LIST OF TABLES

Page

Table 2.1 3σ value based on 202 sets of measurements. 15

Table 4.1 Control limits for energy characteristics in distal depth and distal fall off. 26

Table 4.2 Control limits for energy characteristics in distal depth and distal fall off (cont.). 27

Table 4.3 Control limits for spot characteristics in spot position, spot sigma, spot skewness and spot intensity. 30

Table 4.4 Control limits for spot characteristics in spot position, spot sigma, spot skewness and spot intensity (cont.). 31

Table 4.5 Control limits for uniform field homogeneity, dose output consistency and proton/x-ray coincidence. 41

Table 5.1 Control limits for energy characteristics compared to published literature and TG-224. 43

Table 5.2 Control limits for energy characteristics compared to published literature and TG-224 (cont.). 44

Table 5.3 Control limits for spot characteristics compared to published literature and TG-224. 45

Table 5.4 Control limits for spot characteristics compared to published literature and TG-224 (cont.). 46

Table 5.5 Control limits for x-ray/proton coincidence compared to other published literature and TG-224. 48

Table 5.6 myQA setup for energy characteristics. 50

Table 5.7 myQA setup for spot characteristics. 51

Table 5.8 myQA setup for spot characteristics (cont.). 52

Table 5.9 myQA setup for x-ray/proton coincidence, homogeneity, and dose output consistency. 53

LIST OF FIGURES

Page

Figure 1.1 Integral depth dose function of proton in water. 2

Figure 2.1 Proton interaction mechanisms. 6

Figure 2.2 Integral depth dose function and definition of each position for a proton beam. 7

Figure 2.3 FWHM of proton pencil beam. 8

Figure 2.4 The pencil beam scanning treatment model. 9

Figure 2.5 Component of flat-panel detector. 10

Figure 2.6 Diagram of a parallel plate ion chamber. 11

Figure 2.7 X bar/moving control chart with a central line, upper, and lower control limits. 12

Figure 2.8 The front of QA3 device showing location of ionization chamber and diodes 13

Figure 2.9 (a) The SPREAD phantom on Matrixx-PT. (b) Dimensions of each part of the phantom in centimeters. 14

Figure 2.10 Sphinx Compact measured pristine Bragg peak for proton beam and calculated pristine Bragg peak by TBS. 16

Figure 3.1 Overview of conceptual framework. 18

Figure 3.2 Overview of research design model. 18

Figure 3.3 Varian Compat ProBeam proton treatment system. 19

Figure 3.4 The Sphinx Compact device with all its components; 21

Figure 3.5 Image of Sphinx Compact after performed the daily QA test. 21

Figure 3.6 Sphinx Compact daily QA tasks in different locations. 22

Figure 3.7 myQA software form IBA. 22

Figure 3.8 Sphinx compact, QA plan, and image used to evaluate daily QA data. 23

Figure 4.1 Control chart of distal depth in 100 MeV, 150 MeV, and 200 MeV. 27

Figure 4.2 Control chart of distal fall off in 100 MeV, 150 MeV, and 200 MeV. 28

Figure 4.3 Control chart of proximal depth in 100 MeV, 150 MeV, and 200 MeV. 28

Figure 4.4 Control chart of peak width in 100 MeV, 150 MeV, and 200 MeV. 29

Figure 4.5 Control chart of spot position X of 70 MeV, 100 MeV, and 125 MeV. 32

Figure 4.6 Control chart of spot position X of 150 MeV, 175 MeV, and 200 MeV. 33

Figure 4.7 Control chart of spot position Y of 70 MeV, 100 MeV, 125 MeV, 150 MeV, 175 MeV, and 200 MeV. 34

Figure 4.8 Control chart of spot sigma X of 70 MeV, 100 MeV, 125 MeV, 150 MeV, 175 MeV, and 200 MeV. 35

Figure 4.9 Control chart of spot sigma Y of 70 MeV, 100 MeV, 125 MeV, 150 MeV, 175 MeV, and 200 MeV. 36

Figure 4.10 Control chart of spot skewness X of 70 MeV, 100 MeV, 125 MeV, 150 MeV, 175 MeV, and 200 MeV. 37

Figure 4.11 Control chart of spot skewness Y of 70 MeV, 100 MeV, 125 MeV, 150 MeV, 175 MeV, and 200 MeV. 38

Figure 4.12 Control chart of spot intensity of 70 MeV, 100 MeV, 125 MeV, 150 MeV, 175 MeV, and 200 MeV. 39

Figure 4.13 Control chart of x-ray/proton coincidence in X and Y direction. 41

Figure 4.14 Control chart of uniform field homogeneity. 42

Figure 4.15 Control chart of dose output consistency. 42

Figure 5.1 Comparison of spot energy and % intensity. 47

Figure 5.2 Control chart of x-ray/proton coincidence in X direction. 49

Figure 5.3 Control chart of spot position X of 150 MeV. 49

Figure 5.4 Control chart of spot skewness X of 150 MeV. 49

LIST OF ABBREVIATIONS

AAPM	American Association of In Medicine
CL	Central line
FWHM	Full width at haft-maximum
KCMH	King Chulalongkorn memorial Hospital
kV	kilovolt
LCL	Lower control limit
LET	Linear energy transfer
MeV	megaelectron-volts
MU	Monitor unit
PBS	Pencil beam scanning
PLD	Photoline image document
PPC	Plane-parallel chamber
PPS	Patient positioning system
QA	Quality assurance
QMP	Qualified medical physicist
RBE	Radiobiological effectiveness
ROI	Region of interest
SD	Standard deviations
SOBP	Spread-out Bragg peak

SPC	Statistical process control
TFT	Thin-film transistor
TG	Task group
TPS	Treatment planning system
UCL	Upper control limit
WET	water equivalent thickness

CHAPTER 1

INTRODUCTION

1.1 Background and rationale

Quality assurance (QA) is a systematic procedure for determining whether a product or service fulfills certain specifications. This method assists a corporation in developing products and services that fulfill customer's needs, expectations, and requirements. A quality assurance program's criteria and procedures assist prevent product errors before they arise. The term "quality assurance" in the field of radiation therapy refers to a necessary operation that ensures that the radiation therapy machine is operating as intended for patient treatment and that the planned dosage will be given safely and precisely within tolerance limits. QA is divided into three major categories, according to the American Association of Physicists in Medicine (AAPM): (a) general equipment functionality, (b) patient-specific QA, and (c) treatment planning systems (TPS), with each of these categories further subdivided into daily, weekly, monthly, and annual procedures.

More than 45,000 individuals have recently received radiation therapy involving proton and other charged particle beams for both benign and malignant tumors(1). Proton and other charged particle beams penetrate tissue over a finite distance (defined by particle energy), with the maximal dose deposited near the range's end (the Bragg-peak). The entrance dose is typically 20-25 percent of the peak dose, and there is almost no dose beyond the range's end.

Figure 1.1 shows the relative depth dose of the proton plot with depth. It has 2 main parts: the proximal and the distal part. Proximal id defined by the region before the dose of protons reaches 100% or peak and distal is the region after the peak. Near the surface is the built-up region. It is the first zone in the proximal region, that consists of protonic and electronic buildup. Next to built-up is the sub-peak, which is the zone before the peak. The maximum relative dose is Bragg-peak, and the width of this region is defined by the distance between proximal 80% and distal 80% depth. After the peak is the distal falloff region. The length of this region is defined by the distance at the depth of distal 80% to distal 20%. In this region, the dose will drop off rapidly, this causes the proton beam therapy to have no radiation dose or exit dose to the normal tissue.

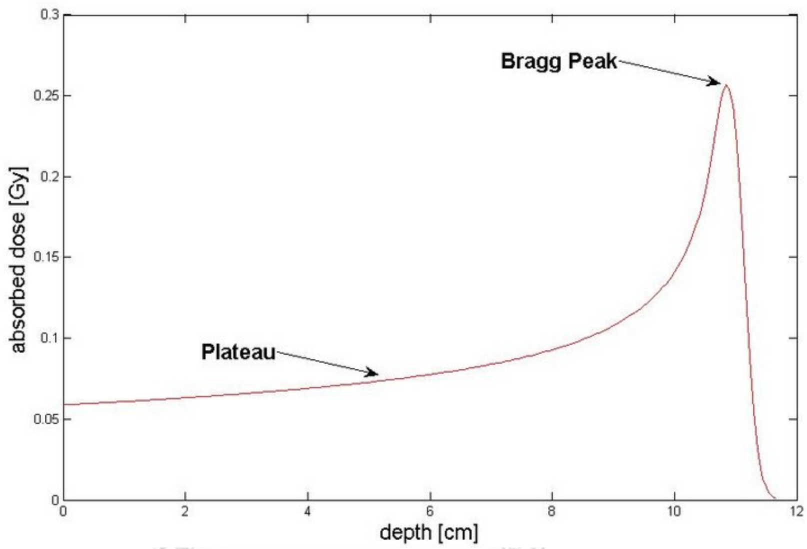

Figure 1.1 Integral depth dose function of proton in water.

A proton pencil beam can be characterized using spot characteristics such as sigma or beam width, skewness, and penumbra. Sigma or beamwidth is the same as proton peak width, which is a distance between proximal 80% to distal 80% depth. The skewness of the proton spot beam is the measure of how much the probability distribution of the proton signal in the spot deviates from the normal distribution. The penumbra or lateral penumbra of the proton spot beam is defined by 80% to 20% distance in spot profile curve.

In modern proton therapy machines, there are two types of proton delivery systems passive and active beam scanning, but the most used type is active beam scanning or pencil beam scanning (PBS). Proton pencil beam scanning is a method of moving a proton beam spot by magnetic scanning while concurrently adjusting the beam intensity, resulting in the dose distribution planned by treatment planning spot by spot, each spot matching to one energy selection spot.(2). Many studies are showing this method can decrease treatment and planning time in many complex cases and is a robust optimization for the treatment planning systems (TPS)(3).

Radiation therapy aims to create the correct uniform dose distribution to a target volume while sparing normal tissues and sensitive structures. To make sure all the processes work properly, there is a standard protocol published by the American Association of Physicists in Medicine (AAPM) which is AAMP TG-224(4). This task group includes all the tasks for quality assurance (QA) on a daily, monthly, and annually. TG-224 focuses on dosimetry and mechanical QA.

From the benefits of proton PBS compared with photon radiation therapy, King Chulalongkorn memorial hospital (KCMH) set up the proton therapy center, Her Royal Highness Princess Maha Chakri Sirindhorn Proton therapy center, and start the first proton therapy treatment in August 2021. This center used the Sphinx Compact® for daily quality assurance checks. The Sphinx Compact is the photo-diode flat-panel detector from IBA® that can be used for both dosimetry and mechanical parts in QA tasks. The principle of flat-panel works by converting the x-ray or proton beams that irradiate on its surface into light and then turning the light into electronic signal or data that computer can display or analyze.

Some studies have shown that the data of daily QA can be evaluated by using a control chart(5, 6) which is a graph used to study how a process changes over time. A qualified medical physicist (QMP) should verify all the results of daily QA procedures and any daily check that is out of tolerance should be immediately reported to the supervising QMP(4).

1.2 Research objective

To establish the baselines of daily QA checks for PBS in the proton therapy at Her Royal Highness Princess Maha Chakri Sirindhorn Proton Therapy center, King Chulalongkorn Memorial Hospital (KCMH) using the Sphinx Compact.

CHAPTER 2
LITERATURE REVIEW

2.1 Theory

Physics of proton therapy

2.1.1 Proton interaction mechanisms

The rest mass of proton is 1832 times that of an electron, causing most of the proton are move in a nearly straight line, and as they pass through matter, they lose kinetic energy through frequent inelastic Coulombic interactions with atomic electrons. On the other hand, A proton passing near to the atomic nucleus experiences a repulsive elastic Coulombic interaction, which deflects the proton off its original straight-line route due to the high mass of the nucleus. Nuclear reactions between protons and atomic nuclei that seem to be non-elastic are less common, but they have more significant effects in nuclear reactions in terms of individual protons(7). The projectile proton enters the nucleus; the nucleus may emit a proton, deuteron, triton, or heavier ion. In theory, proton Bremsstrahlung is possible, but at therapeutic proton beam energies, the effect is negligible.

Figure 2.1 illustrates the proton interaction mechanisms; (*a*) Coulombic interaction with inelastic energy loss, (*b*) repulsive deflection of proton trajectory nucleus coulomb elastic scattering, (*c*) non-elastic nuclear interaction by remove the primary proton and create secondary particles. (Proton: p, Electron: e, Neutron: n, gamma rays: γ)

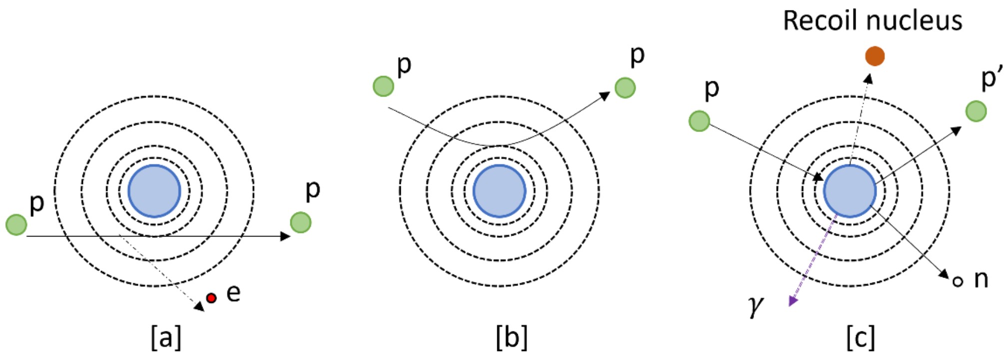

Figure 2.1 Proton interaction mechanisms.

2.1.2 Proton Bragg peak curve

When protons travel through the matter, each interaction is generally a very small amount of each particle kinetic energy loss. The protons are continuously slowing down until they completely stop. The quotient of dE and dX, where E is the mean energy loss and X is the distance, is the energy loss rate of ions, or linear stopping power. This rate of energy loss can be stated in a form that is unaffected by mass density; the mass stopping power is defined as $\frac{S}{\rho} = -\frac{dE}{\rho dx}$ where ρ is the mass density of the absorbing material. The stopping power increases as a proton slows down that causes a proton loses a large amount of its energy immediately before the particle comes to rest creating a dose deposition peak at the end of the proton range called Bragg peak as presented in figure 2.2.

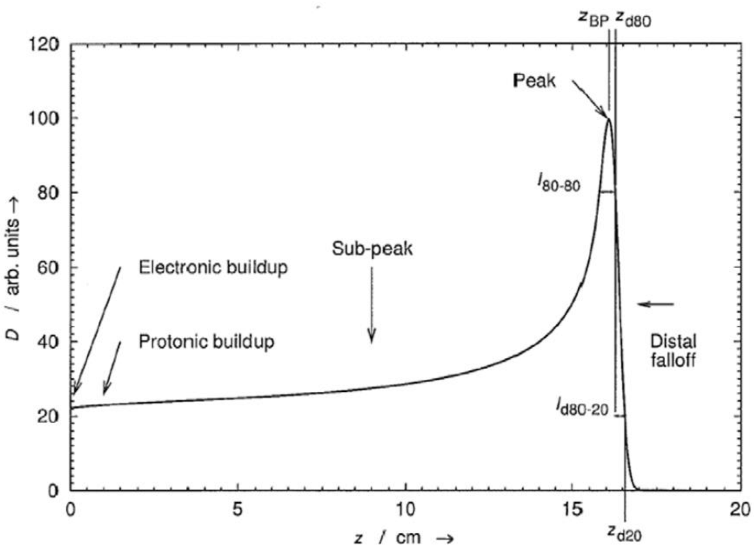

Figure 2.2 Integral depth dose function and definition of each position for a proton beam.

Electronic buildup region is the small region near the surface of the absorber where the proton beam is incident. Delta rays with plenty of kinetic energy to travel several millimeters in tissue are liberated by high-energy proton beams(7). With increasing depth, the dose in this region increases. In some cases, this region is not observed.

Protonic buildup region is the region near the surface of the absorber where absorber dose increases with depth due to the buildup of secondary protons that are attributable to proton-induced non-elastic nuclear interaction(7).

Sub-peak region is the region extending from the absorber's surface to the depth closest to the peak

Pristine Bragg peak is the maximum dose near the end of the proton range. The proton stopping power is primarily responsible for determining the location and height of the peak.

Pristine Bragg peak depth is the depth near the end of range of the protons at which the protons create the maximum dose rate.

Distal falloff region is the region behind the depths greater than pristine Bragg peak depth.

80%-to-20% distal falloff length is the distance between 80% distal and 20% distal depth.

80% proximal-to-80% distal pristine-peak width is the distance between 80% proximal depth and 80% distal depth.

For spot profile, the full width at half-maximum (FWHM) of the pencil beam, or one sigma of its approximate Gaussian representation, measured at a specific position in air or water, where relationally FWHM = 2.35 (4) as shown in figure 2.3

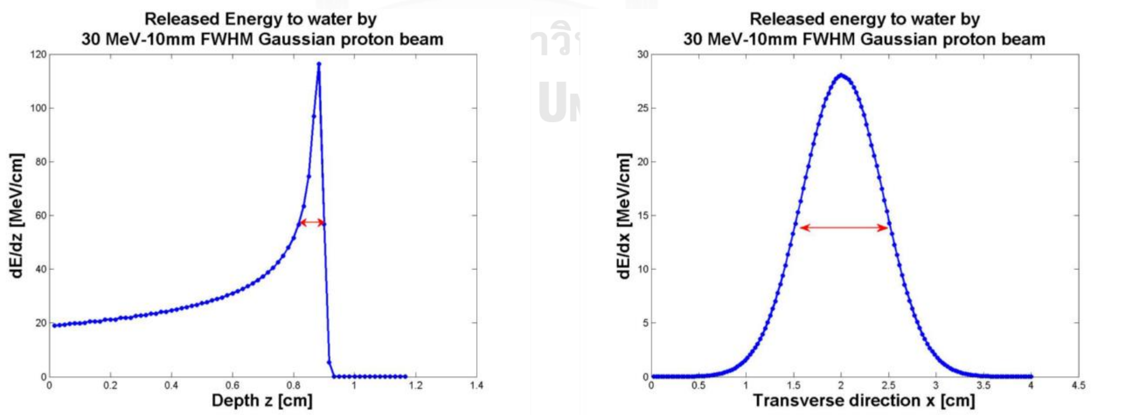

[a] [b]

Figure 2.3 FWHM of proton pencil beam.

(a) parallel (longitudinal) to the beam direction, (b) perpendicular (transverse) to the beam direction(8)

2.1.3 Proton pencil beam scanning

Proton pencil beam scanning or active scanning is the most used method for proton beam delivery systems. Figure 2.4 shows a schematic view of proton pencil beam scanning. The concept is to use a pencil beam of the proton which is a narrow-controlled beam of proton particles to treat tumor or target volume in the patient. The tumor or 3D target volume is divided into several slices or layers which can be determined by proton initial energy, each layer is a collection of a mono-energetic spot of various positions of the proton pencil beam. The direction of each proton spot, a collection of mono-energetic proton that is deposited at a given position, controlled by bending the spot beam to the target location by the magnetic scanner. Pencil beam scanning can be separated into two types: spot scanning and continuous scanning. Irradiating one specific point in a volume depositing is called spot scanning. Turning off the beam and going to the next location, turning on the beam, and then irradiating that location to achieve the appropriate dose. The beam stays on while the spot moves in continuous scanning, and the dose at any particular point is governed by the beam current and/or the speed of the beam's travel.

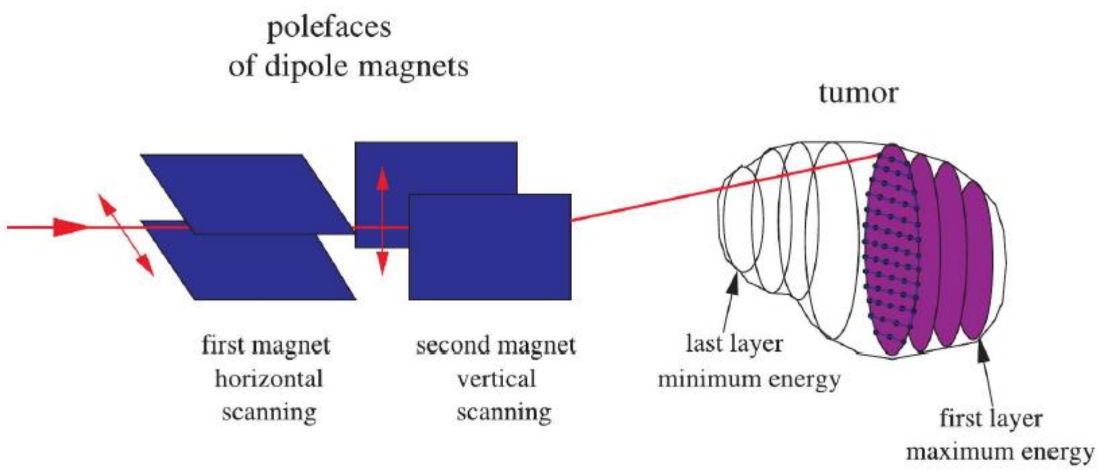

Figure 2.4 The pencil beam scanning treatment model.

Radiation dosimeter

2.1.4 Flat-panel detector

The flat-panel detector converts the X-rays or proton beam that irradiate its surface into light, which is subsequently converted into electronic data that the computer can display or analyze. Components of the flat-panel detector are shown in figure 2.5. A layer of scintillator material is present in this detector, which turns the radiation into light. Millions of around 0.2 mm pixels are printed in amorphous silicon on the glass substrate behind the scintillator layer, each containing a thin-film transistor (TFT). Each pixel has a photodiode that produces an electrical signal proportional to the amount of light produced by the scintillator layer in front of it. Additional electronics positioned at the edges or behind the sensor array amplifies and encodes the signals from the photodiodes to provide an accurate and sensitive digital representation of the radiation(9).

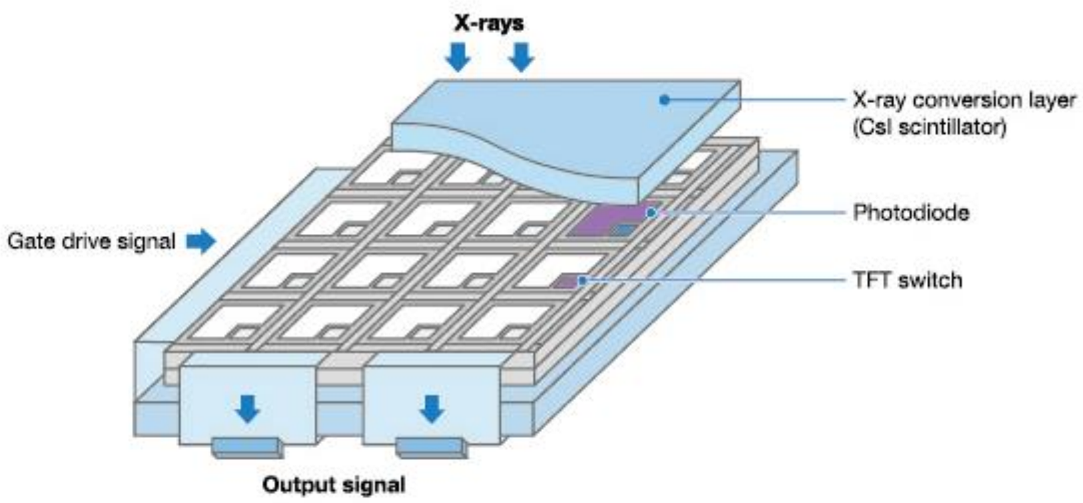

Figure 2.5 Component of flat-panel detector.

2.1.5 Ionization chamber detector

The ionization chamber is a gas-filled radiation detector that is commonly used for the detection and measurement of X-ray, gamma-ray, and charged particle ionizing radiation. A gas ionization chamber calculates the charge from the number of ion pairs generated by incoming radiation within a gas. It is made up of a gas-filled chamber and two electrodes called the cathode and anode. Between the field in the filled gas and the voltage potential is applied. Ion-pairs are formed when incident ionizing radiation ionizes the gas between the electrodes, and the positive ions and dissociated electrons migrate to the electrodes of the opposite polarity under the influence of the electric field. An electrometer circuit measures the ionization current that is generated. Each ion pair formed deposits or removes a little electric charge from the electrode, accumulating a charge proportionate to the number of ion pairs formed, and hence the radiation dose. The ionization current, which is a measure of the total ionization dose entering the chamber, is produced by this continuous creation of charge(10). The diagram of parallel ion chamber is shown in figure 2.6

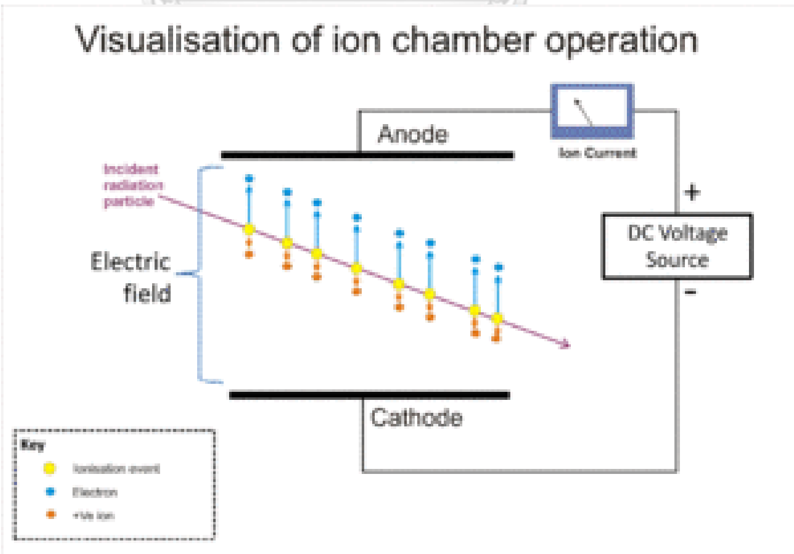

Figure 2.6 Diagram of a parallel plate ion chamber.

2.1.6 X bar/moving range control chart

X bar/moving range (X/mR) chart is a control chart for processes with a subgroup size of one. This chart is used to monitor the stability of the process and characterize the systematic error from random error. The chart creates a picture of how the system change over time as shown the example in figure 2.7. X-bar is the average of measurement, and moving range is variability between one data point to the next point. The three main parts of control chart are central line (CL) which represents the average of measurement, upper and lower control limits (UCL, LCL) are the two horizontal lines calculated from mean of moving range of the measurement. This chart can be set to be baselines of measurement data which used for comparison with later data.

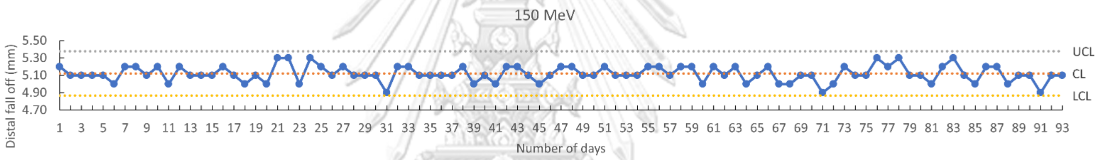

Figure 2.7 X bar/moving control chart with a central line, upper, and lower control limits.

2.2 Review of related literature

2.2.1 Lambert J. et al. (2014) developed an innovative method for using a single device for daily proton pencil beam scanning quality assurance (QA). Sun Nuclear QA3 (Melbourne, FL) device for routine QA in photon/electron radiation beams (Figure 2.8). It has been modified to measure the X-ray system's range, output, and collinearity, as well as the proton beam, spot position, and spot sigma. The PBS beam's output result has maintained under the 2% tolerance, and nearly all measurements are within 1% of the baseline. The range's stability has remained within 1 mm. In all QA measures, the spot position is within 1 mm of the baseline position. The Y-axis spot sigma was initially unpredictable, with deviations exceeding the tolerance of 15%. This research found that this approach may be used to assess spot position accuracy and sigma in a PBS beam, as well as range accuracy and output in any proton therapy beam, all in a single irradiation.

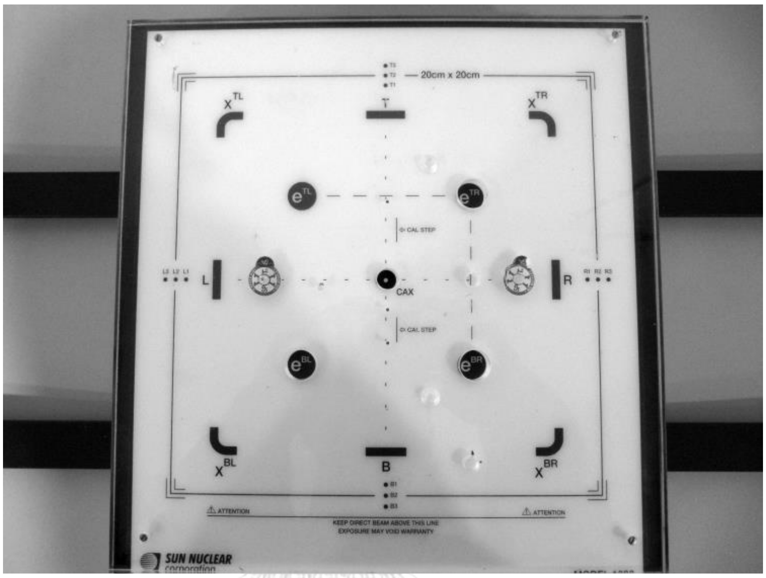

Figure 2.8 The front of QA3 device showing location of ionization chamber and diodes.

2.2.2 Bizzocchi N. et. al. (2017) developed, manufactured, and tested a new phantom with an array of ionization chambers that lowered execution times while retaining test reliability. Two pairs of wedges were provided to the SPREAD phantom to sample Bragg-peak at different depths. As shown in figure 2.9, three 'boxes' are used to check spot positioning and deliver dose. The test revealed excellent reproducibility of spot characteristics after one month of use. According to the findings, this QA equipment can correctly detect 98 percent of spots that are inside the 1 mm tolerance for spot location and 99 percent of spots that are beyond the tolerance. All range deviations of more than 2 mm were identified successfully.

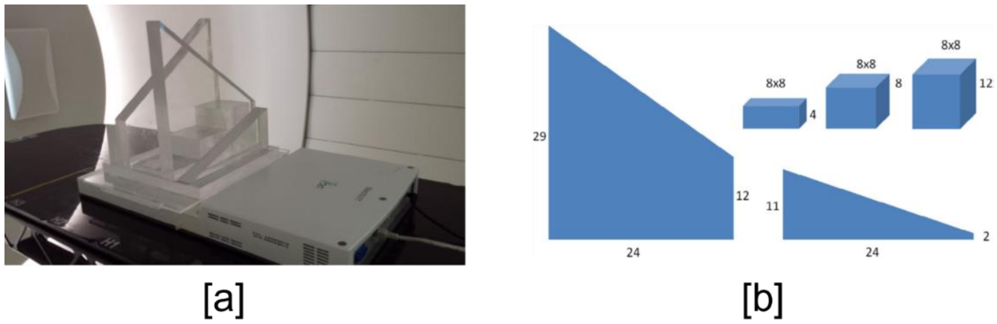

Figure 2.9 (a) The SPREAD phantom on Matrixx-PT. (b) Dimensions of each part of the phantom in centimeters.

2.2.3 Rena S. et. al. (2019) demonstrated the clinical implementation of comprehensive pencil beam scanning daily quality assurance program by using novel QA device Sphinx, Lynx, and parallel-plate (PPC05) ion chamber. The daily QA of spot position, spot sigma, spot skewness, distal range, distal fall-off, peak width, imaging vs proton beam isocenter coincidence, field homogeneity, and dose output were performed. All these data were analyzed by myQA software form IBA dosimetry and evaluated the baselines using statistical process control (SPC) of Xbar/R control chart. Xbar/R control charts are the chart created using the mean value, upper and lower control limits which are defined by +/- 3σ (sigma or standard error of average value). Three times of standard error cover 99.73% of values lie within 3 standard deviations (S.D.) of mean. Results of using Xbar/R control chart showed that upper and lower control limits can be used to determine if individual measurements required action. Table 2.1 is ±3σ based on control chart of this study.

Table 2.1 3σ value based on 202 sets of measurements.

Daily QA tests	**3σ based on control chart**
Dose output	±0.7%
Field homogeneity	±0.5%
Distal range	±0.3 mm
Proximal range	±0.2 mm
Width	±0.2 mm
Distal fall-off	± 0.1 mm
Beam coincidence X	±0.7 mm
Beam coincidence Y	±0.5 mm
Spot position X	±0.6 mm
Spot position Y	±0.4 mm
Spot sigma X	±2.1%
Spot Sigma Y	±3.6%
Skewness X	±0.3
Skewness Y	±0.3

2.2.4 Su Z. et. al. (2020) evaluated flat-panel detector, sphinx compact®, quenching effect and usability of flat-panel based compact detector, sphinx compact, QA device for use in PBS constancy measurement. In Bragg-peak region some of radiation detector will show an underestimation result when irradiated by proton beam(11, 12). Using Sphinx Compact to measure the depth dose of mono-energetic proton beam through increments of solid water slabs (RW3) of the different thickness in front of the detector. Figure 2.10 showing that the distal R80 value in water equivalent thickness (WET) of measure curves were within 1 mm. The quenching effect of the detector is an effect that makes the signal level reduced significantly when the detector is close to Bragg-peak where the linear energy transfer (LET) for proton is very high. The different between measurement and TPS indicating that Sphinx Compact can be used for proton range measurement and LET dependent quenching effect in Bragg peak region did not have an impact on the daily QA constancy test.

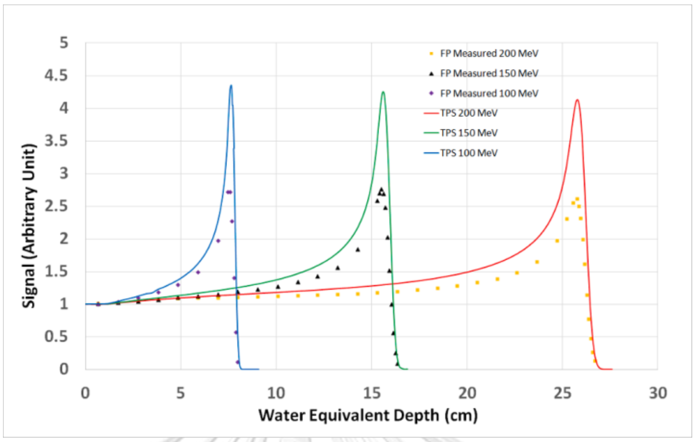

Figure 2.10 Sphinx Compact measured pristine Bragg peak for proton beam and calculated pristine Bragg peak by TBS.

To evaluate the usability of the sphinx compact®, characteristics of the detector were determined using 3 proton energies of 100, 150 and 200 MeV representing low, medium, and high energies after the detector has been characterized. The daily QA tests as published by AAMP TG-224(4) were spot characteristics, flatness, uniform field homogeneity, laser alignment, energy consistency, output dose consistency, patient positioning system (PPS) displacement, and proton/x-ray coincidence. This study concluded that Sphinx Compact device provided the flexibility to the user of their PBS daily QA checks recommended by AAPM TG-224 protocol.

According to the literature reviews, the baselines of daily QA for proton pencil beam scanning should be evaluated and reviewed because there is no available or established report about the baselines for proton therapy center earlier at KCMH, Thailand. These baselines can be a useful tool to monitor each of the daily QA data for the proton therapy center, and the Sphinx Compact has shown a flexibility and comprehensive use for daily QA checks which will help the user perform daily QA more efficiently with less setup and less time to evaluate.

CHAPTER 3

RESEARCH METHODOLOGY

3.1 Research design

This study is descriptive with a prospective study.

3.2 Conceptual framework

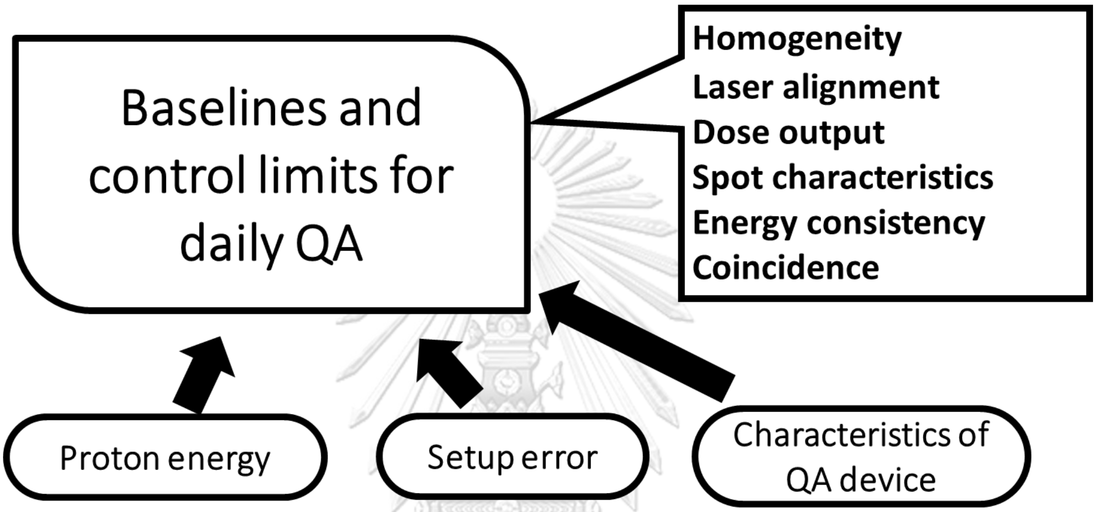

Figure 3.1 Overview of conceptual framework.

3.3 Research design model

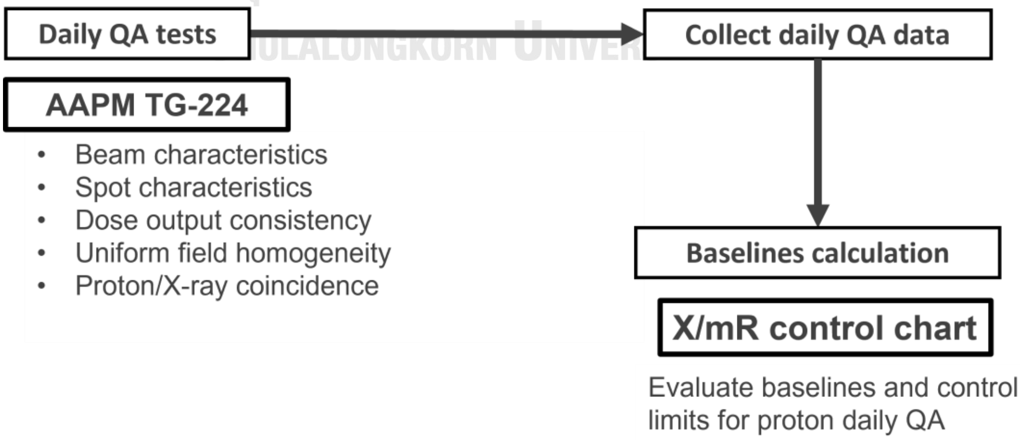

Figure 3.2 Overview of research design model.

3.4 Research question

What are the baselines of daily QA checks for proton PBS in the proton therapy center at Her Royal Highness Princess Maha Chakri Sirindhorn Proton Therapy center, KCMH, using the Sphinx Compact detector?

3.5 Research objective

To establish the baselines for daily QA checks for proton PBS at Her Royal Highness Princess Maha Chakri Sirindhorn Proton Therapy center, KCMH, using the Sphinx Compact detector.

3.6 Materials

3.6.1 Proton therapy system

Figure 3.3 is the ProBeam Compact (Varian Medical System, Palo, Alto, CA) with a PBS delivery system that generates protons from a cyclotron with energies ranging from 70 MeV up to 250 MeV with fully 360° gantry rotation and a robotic treatment couch. The kV x-ray imaging system consists of two x-ray tubes and two planar detectors that are capable of performing 2D, 3D, and cone-beam CT (CBCT) image-guided proton treatment.

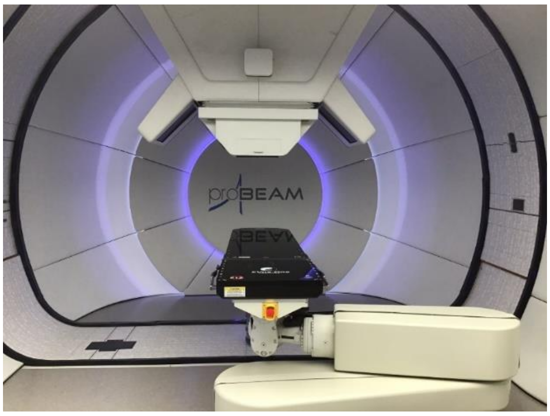

Figure 3.3 Varian Compat ProBeam proton treatment system.

3.6.2 Sphinx Compact QA device

Sphinx Compact (IBA dosimetry, Schwarzenbruck, Germany) is the photodiode flat panel detector that has a 20x20 cm^2 active area detector made of amorphous silicon, and a resolution of 0.2 mm. A carbon fiber frame, a high-resolution photo-diode type flat-panel imager, and a group of block modules constructed of high-density plastic material in various shapes make up this detector, as illustrated in figure 3.4. The carbon fiber frame supports the flat-panel imager. Three energy test blocks are included in the block modules. The wedge block for measuring the spread-out Bragg peak or SOBP profile and a block accommodating a PPC05 plane-parallel chamber (IBA dosimetry, Schwarzenbruck, Germany) connecting with Dose 1 electrometer (IBA dosimetry, Schwarzenbruck, Germany) for machine output measurements. One gradient surface faces the proton beam on each of the three energy blocks and wedge blocks. The pixel charge amplifiers' capacitance is directly proportional to the detector's gain settings (0.25, 0.5, 1, 2, 4, and 8 pF). The bigger capacitance allows for a higher charge count reading without the charge amplifier becoming saturated(6).

Sphinx Compact can be measured the uniform field homogeneity, output dose consistency, proton/ X-ray beam isocenter coincidence and beam characteristics, which can be divided into energy and spot characteristics. Energy characteristics are distal depth, proximal depth, distal falloff, and peak width. Spot characteristics are spot position, spot sigma, or spot size, spot skewness, which indicates how circular the spot is, and spot intensity.

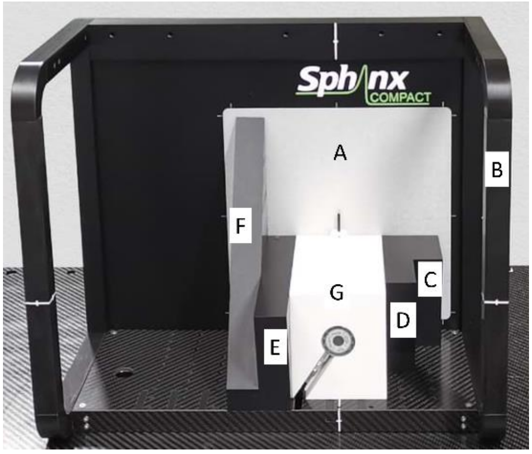

Figure 3.4 The Sphinx Compact device with all its components; (A) flat-panel imager, (B) transportation frame, (C) energy test module for 100 MeV proton, (D) energy test module for 150 MeV proton, (E) energy test module for 200 MeV proton, (F) SOBP wedge module and (G) PPC05 output test module.

The image of daily QA test shown in figure 3.5 and figure 3.6 shows the location of each daily QA tasks.

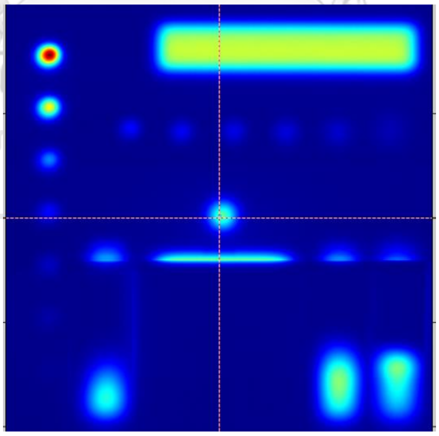

Figure 3.5 Image of Sphinx Compact after performed the daily QA test.

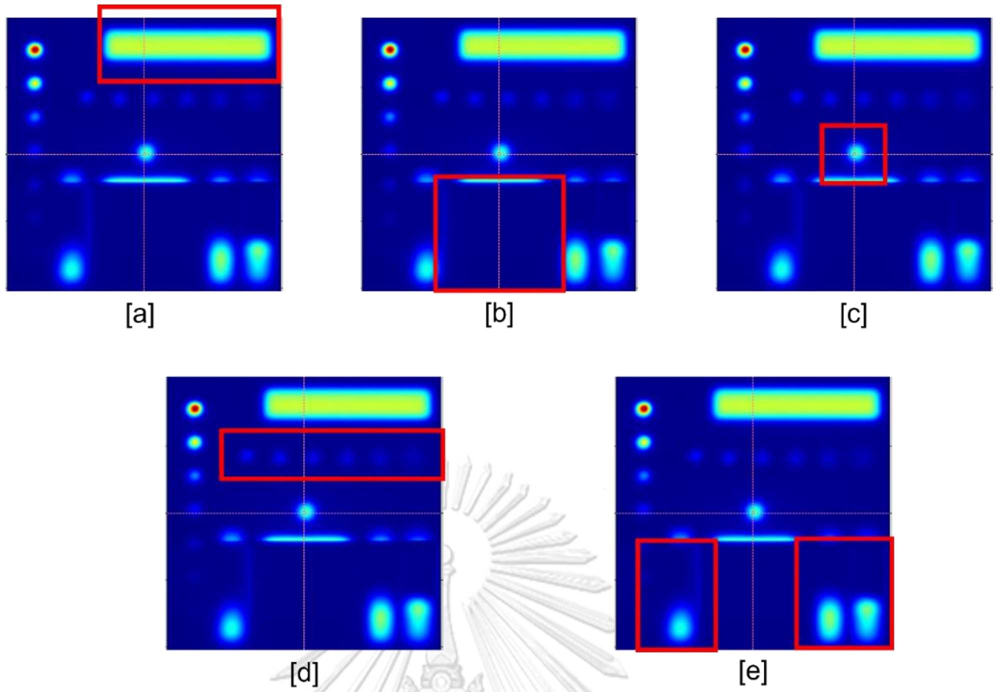

Figure 3.6 Sphinx Compact daily QA tasks in different locations.

(a) Uniform field homogeneity, (b) Output dose consistency, (c) x-ray/proton coincidence, (d) spot characteristics, (e) energy characteristics.

3.6.3 myQA software

The myQA software version 2020-001 (2.13.14.0) (IBA dosimetry, Schwarzenbruck, Germany) as shown in figure 3.7, was used to analyze all the daily QA data performed by Sphinx Compact.

Figure 3.7 myQA software form IBA.

3.7 Methods

3.7.1 Daily QA test of proton pencil beam scanning

The Sphinx Compact, PPC05 detector, and myQA software were used to perform the daily QA test from September 23rd until December 29th, 2021. The QA plan was created according to Sphinx Compact instructions and imported into myQA software to use for evaluating the daily QA data. QA plans use 3 proton energies; 100 MeV, 150 MeV, and 200 MeV for energy characteristics including distal depth, distal fall off, proximal depth, and proton peak width. The 6 proton energies; 100 MeV, 125 MeV, 150 MeV, 175 MeV, and 200 MeV are used for spot characteristics, including spot position, spot sigma or spot size, spot skewness, and spot intensity.

These QA plans also include a task for beam flatness (homogeneity of the beam), X-ray/proton coincidence and dose output consistency as instructed by AAPM TG-224(4). All the results were recorded to evaluate baselines for daily QA tasks. Comparison between Sphinx Compact, PLD file, and image after performed daily QA test shown in figure 3.8

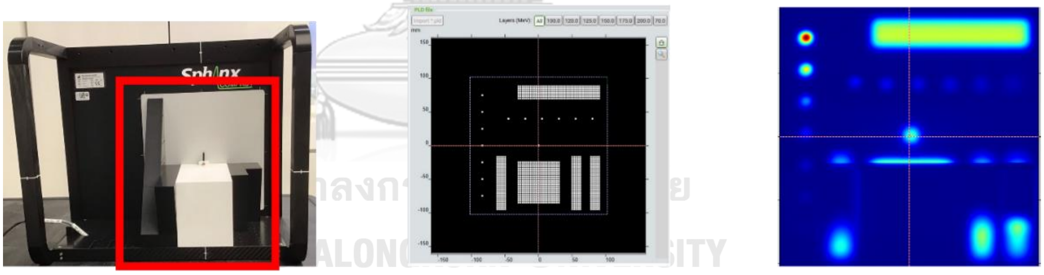

[a] [b] [c]

Figure 3.8 Sphinx compact, QA plan, and image used to evaluate daily QA data. (a) imager of Sphinx compact, (b) PLD file used in myQA software, (c) image after performed daily QA test

3.8 Statistical analysis

3.9.1 Statistical process control (SPC)

X/mR (x bar/moving range) control chart was used to evaluate baselines of daily QA tests. The upper and lower control limits were calculated using the following equations.

$$Upper\ control\ limit = \bar{x} + 3(X_{indi})$$
$$Lower\ control\ limit = \bar{x} - 3(X_{indi})$$

$\bar{x}$ = average values

X_{indi} = sequential standard deviation

For moving range, mean of absolute difference between sequential measurement (mR) was calculated, then the sequential standard deviation (X_{indi}) was calculated by this equation.

$$X_{indi} = \frac{mean\ (mR)}{1.128}$$

X_{indi} = sequential standard deviation

mR = absolute difference between sequential measurement

3.9 Data analysis

Data was reported as upper and lower control limits of each daily QA task, presented in the form of a table and an X/mR control chart.

3.10 Outcome

Baselines and control limits for daily QA in proton pencil beam scanning at Her Royal Highness Princess Maha Chakri Sirindhorn Proton Therapy center, KCMH.

3.11 Expected benefits

The results of this study can be used to be the baselines and control limits of daily QA at Her Royal Highness Princess Maha Chakri Sirindhorn Proton Therapy center, KCMH.

3.12 Limitation

This study used previous data of daily QA to evaluate the baselines. When the data are out-of-limit zone, it can't be fixed or reperformed the daily QA tasks immediately.

3.13 Ethical consideration

This study was submitted to the Institutional Review Board (IRB) of the faculty of Medicine, Chulalongkorn University, Bangkok, Thailand. The committee confirmed that ethics is not required because there is no human subject involved in any part of the study.

CHAPTER 4
RESULTS

4.1 Energy characteristics

Energy characteristics including distal depth, proximal depth, distal falloff, and peak width for 3 proton energies were measured. The average value, upper control limit and lower control limit were calculated using 50 daily QA data for each task. Control limits in each test are shown in table 4.1 For distal depth, the upper and lower control limits for 100 MeV, 150 MeV and 200 MeV were ± 0.1 mm, ± 0.3 mm, and ± 0.5 mm, respectively. For distal falloff, the upper and lower control limits for 100 MeV, 150 MeV and 200 MeV were ± 0.2 mm, 0.3 mm, and 0.5 mm, respectively. For proximal depth, the upper and lower control limits for 100 MeV, 150 MeV and 200 MeV were ± 0.4 mm, ± 0.3 mm, and ± 0.5 mm, respectively. For peak width, the upper and lower control limits for 100 MeV, 150 MeV and 200 MeV were ± 0.4 mm, ± 0.4 mm, and ± 0.5 mm, respectively.

Table 4.1 Control limits for energy characteristics in distal depth and distal fall off.

Parameters	Energy (MeV)	Average (mm)	Control limits (mm)
Distal depth	100	75.7	± 0.1
	150	155.9	± 0.3
	200	257.0	± 0.5
Distal fall off	100	3.0	± 0.2
	150	5.1	± 0.3
	200	6.0	± 0.5

Table 4.2 Control limits for energy characteristics in distal depth and distal fall off (cont.).

Parameters	Energy (MeV)	Average (mm)	Control limits (mm)
Proximal depth	100	69.4	± 0.4
	150	147.5	± 0.3
	200	251.1	± 0.5
Peak width	100	6.3	± 0.4
	150	8.4	± 0.4
	200	5.9	± 0.5

Control charts of energy characteristics are shown in figures 4.1 – 4.4. All the control charts were calculated using 50 data of each daily QA test shown in white dots in the graph and used these baselines to apply to the rest of the daily QA data.

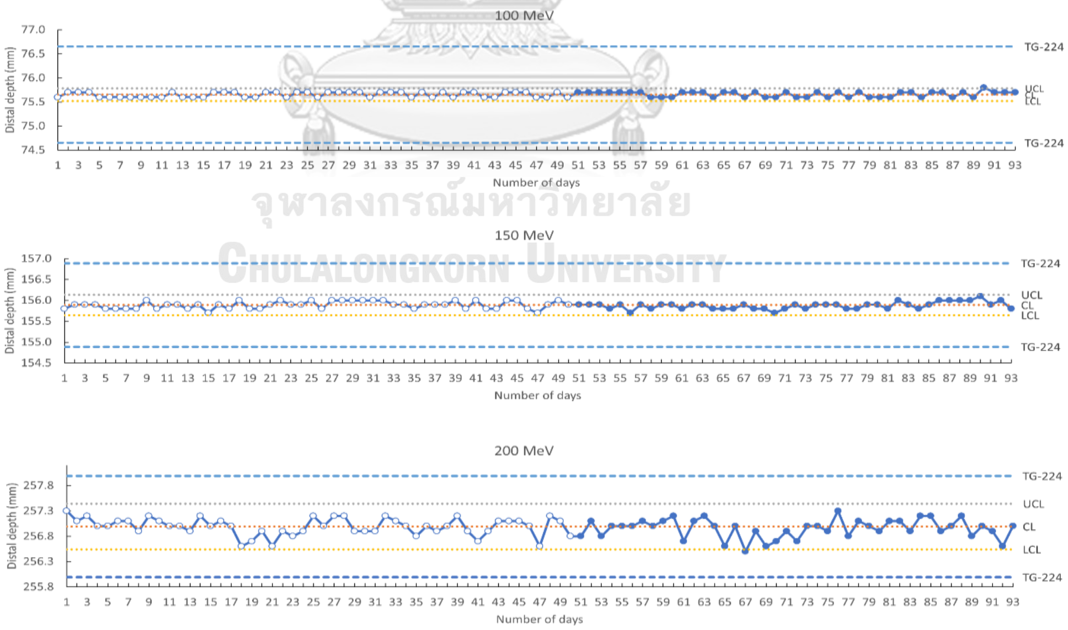

Figure 4.1 Control chart of distal depth in 100 MeV, 150 MeV, and 200 MeV.

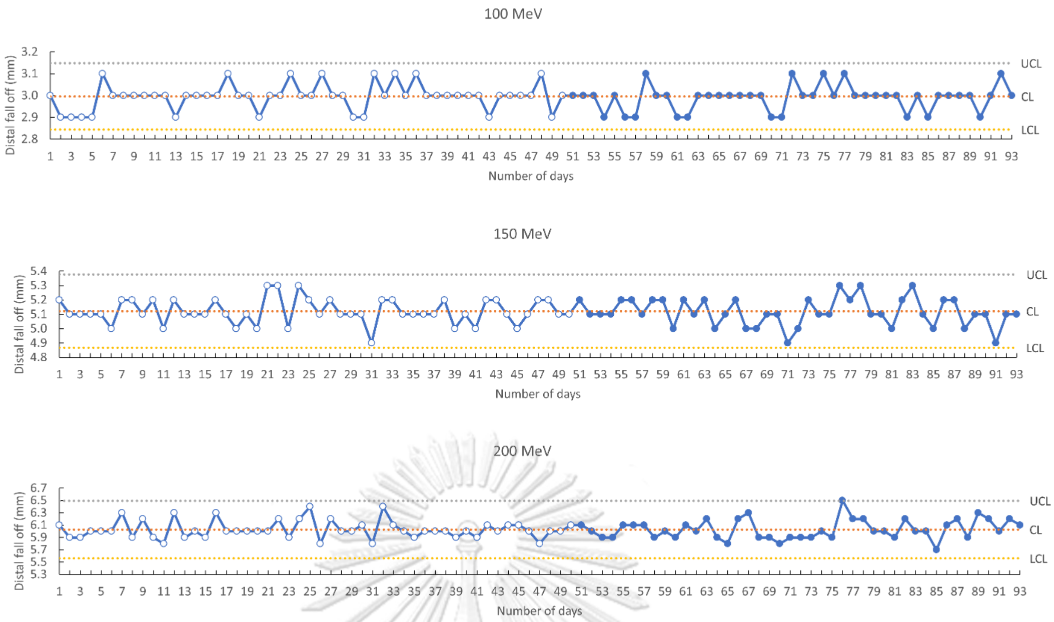

Figure 4.2 Control chart of distal fall off in 100 MeV, 150 MeV, and 200 MeV.

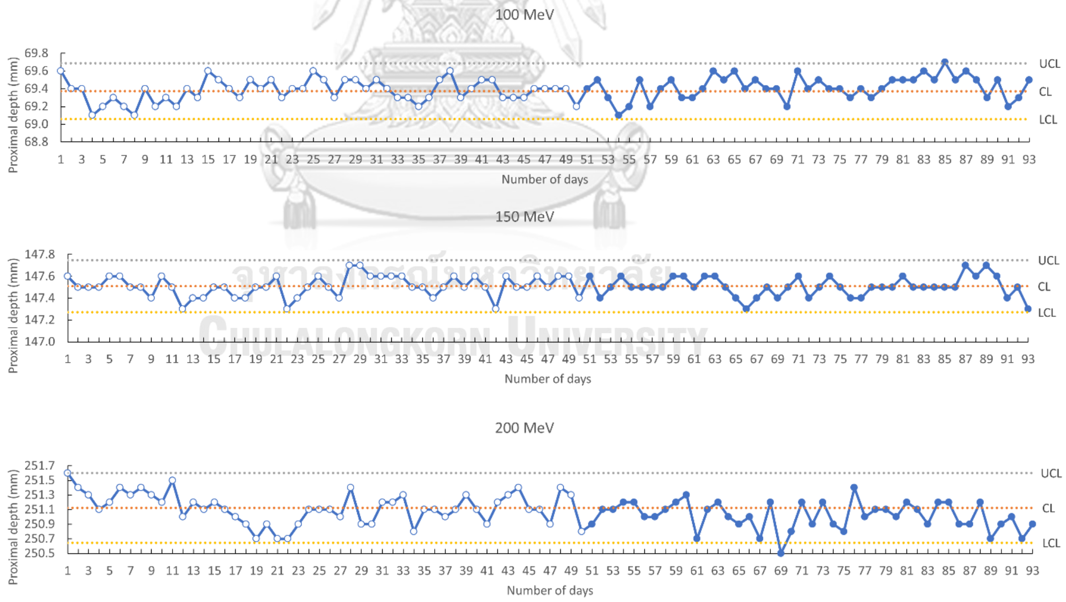

Figure 4.3 Control chart of proximal depth in 100 MeV, 150 MeV, and 200 MeV.

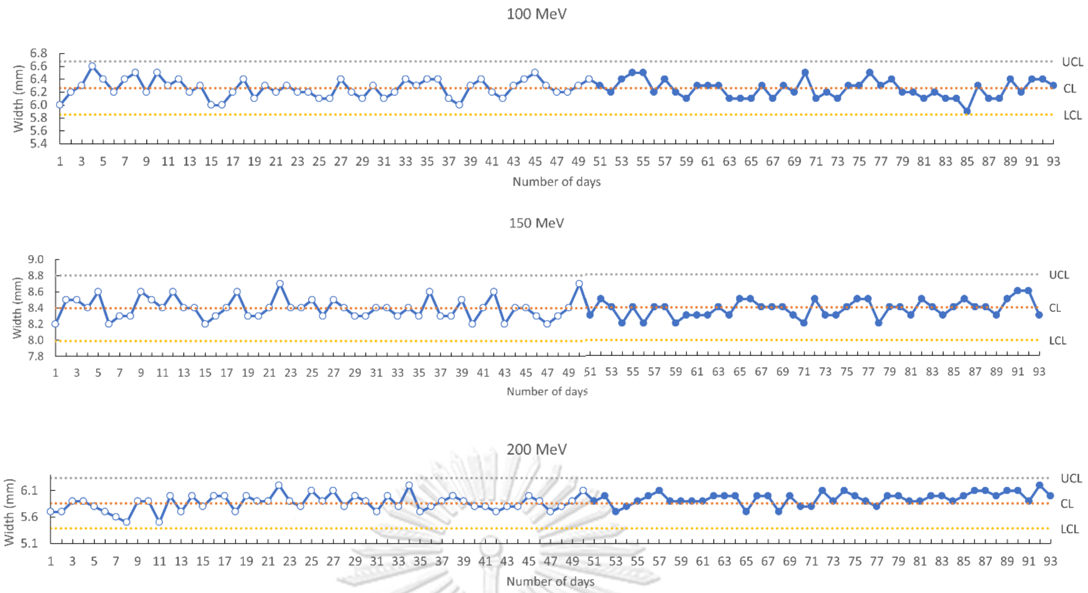

Figure 4.4 Control chart of peak width in 100 MeV, 150 MeV, and 200 MeV.

4.2 Spot characteristics

Spot characteristics including spot position in X and Y directions, spot sigma in X and Y directions, spot skewness in X and Y directions and spot intensity for 6 proton energies. The average value, upper control limit and lower control limit were calculated using 50 of daily QA data for each task. Table 4.2 shows control limits of each test. For spot position, the upper and lower control limits for 70 MeV, 100 MeV, 125 MeV, 150 MeV, 175 MeV, and 200 MeV were ± 1.0 mm, ± 0.7 mm, ± 0.8 mm, ± 0.8 mm, ± 0.7 mm, and ± 1.2 mm in X direction and ± 0.5 mm, ± 0.5 mm, ± 0.4 mm, ± 0.7 mm, ± 0.5 mm and ± 0.8 mm in Y direction, respectively. For spot sigma, the upper and lower control limits for 70 MeV, 100 MeV, 125 MeV, 150 MeV, 175 MeV, and 200 MeV were ± 2.0 mm, ± 1.3 mm, ± 1 mm, ± 0.9 mm, ± 0.8 mm, and ± 0.8 mm in X direction and ± 2.9 mm, ± 1.4 mm, ± 1.3 mm, ± 1.3 mm, ± 1.1 mm, and ± 1.1 mm in Y direction, respectively. For spot skewness, the upper and lower control limits for 70 MeV, 100 MeV, 125 MeV, 150 MeV, 175 MeV, and 200 MeV were ± 0.380, ± 0.315, ± 0.333, ± 0.357, ± 0.334, and ± 0.621 in X direction and ± 0.119, ± 0.191, ±

0.175, ± 0.222, ± 0.175, and ± 0.394 in Y direction, respectively. For spot intensity, the upper and lower control limits for 70 MeV, 100 MeV, 125 MeV, 150 MeV, 175 MeV, and 200 MeV were ± 1.5 %, ± 1.4 %, ± 1.5 %, ± 1.8 %, ± 1.8 %, and ± 1.0 %, respectively.

Table 4.3 Control limits for spot characteristics in spot position, spot sigma, spot skewness and spot intensity.

Parameters	Energy (MeV)	Average (mm)	Control limits (mm)
Spot position X	70	80.6	± 1.0
	100	55.6	± 0.7
	125	30.8	± 0.8
	150	5.5	± 0.8
	175	-19.2	± 0.7
	200	-44.5	± 1.2
Spot position Y	70	42.0	± 0.5
	100	41.3	± 0.5
	125	41.2	± 0.4
	150	41.2	± 0.7
	175	41.2	± 0.5
	200	41.8	± 0.8
Spot sigma X	70	7.7	± 2.0
	100	5.9	± 1.3
	125	5.2	± 1.0
	150	4.8	± 0.9
	175	4.4	± 0.8
	200	4.2	± 0.8

Table 4.4 Control limits for spot characteristics in spot position, spot sigma, spot skewness and spot intensity (cont.).

Parameters	Energy (MeV)	Average	Control limits
Spot sigma Y	70	8.0 mm.	± 2.9 mm.
	100	6.9 mm.	± 1.4 mm.
	125	5.4 mm.	± 1.3 mm.
	150	4.9 mm.	± 1.3 mm.
	175	4.5 mm.	± 1.1 mm.
	200	4.0 mm.	± 1.1 mm.
Spot skewness X	70	0.366	± 0.380
	100	0.223	± 0.315
	125	0.324	± 0.333
	150	0.361	± 0.357
	175	0.286	± 0.334
	200	0.372	± 0.621
Spot skewness Y	70	0.653	± 0.119
	100	0.428	± 0.191
	125	0.408	± 0.175
	150	0.389	± 0.222
	175	0.414	± 0.175
	200	0.592	± 0.394
Spot intensity	70	5.4 %	± 1.5 %
	100	7.4 %	± 1.4 %
	125	9.1 %	± 1.5 %
	150	10.5 %	± 1.8 %
	175	11.7 %	± 1.8 %
	200	13.2 %	± 1.0 %

Control charts of each energy characteristics are shown in figures 4.5 – 4.12. All the control charts were calculated using 50 data of each daily QA test shown in white dots in the graph and used these baselines to apply to the rest of the daily QA data. On date number 11, 12, and 13, the results of x-ray/proton coincident were in out of limit zone as shown in figure 4.13. These 3 days were excluded and present in the red dots in control chart from each spot characteristics daily QA test for baselines calculation.

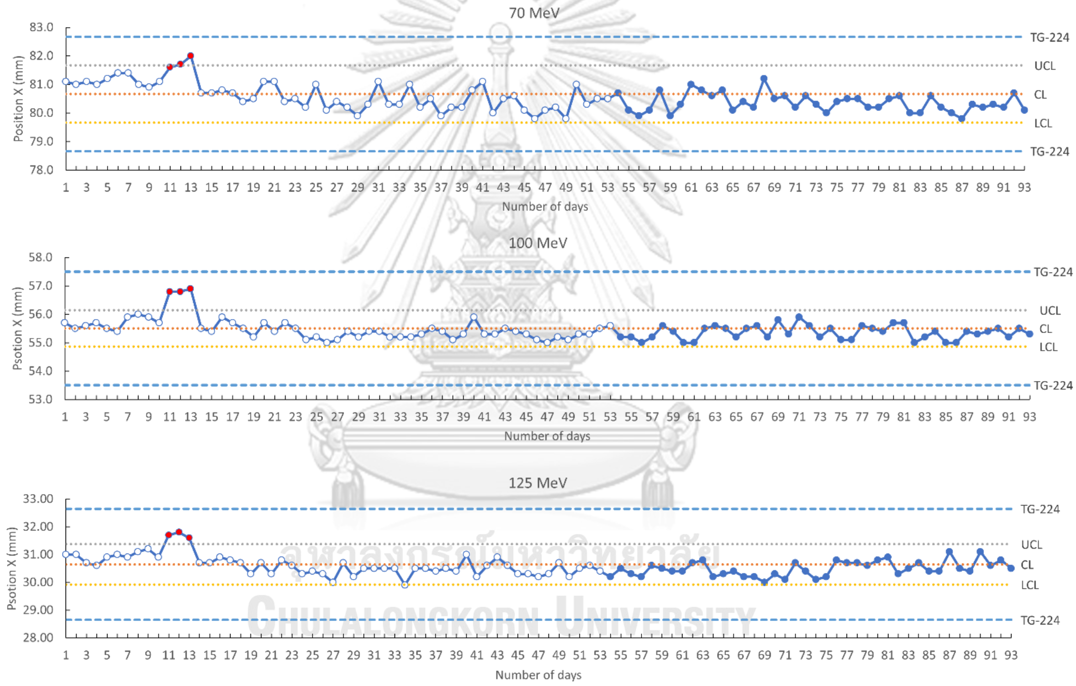

Figure 4.5 Control chart of spot position X of 70 MeV, 100 MeV, and 125 MeV.

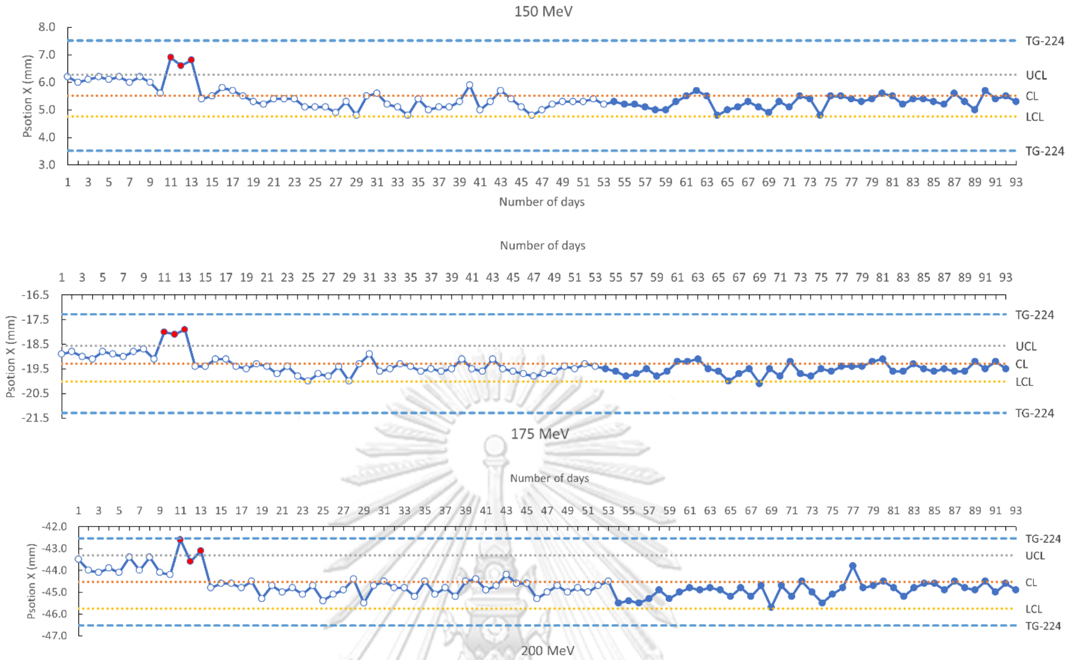

Figure 4.6 Control chart of spot position X of 150 MeV, 175 MeV, and 200 MeV.

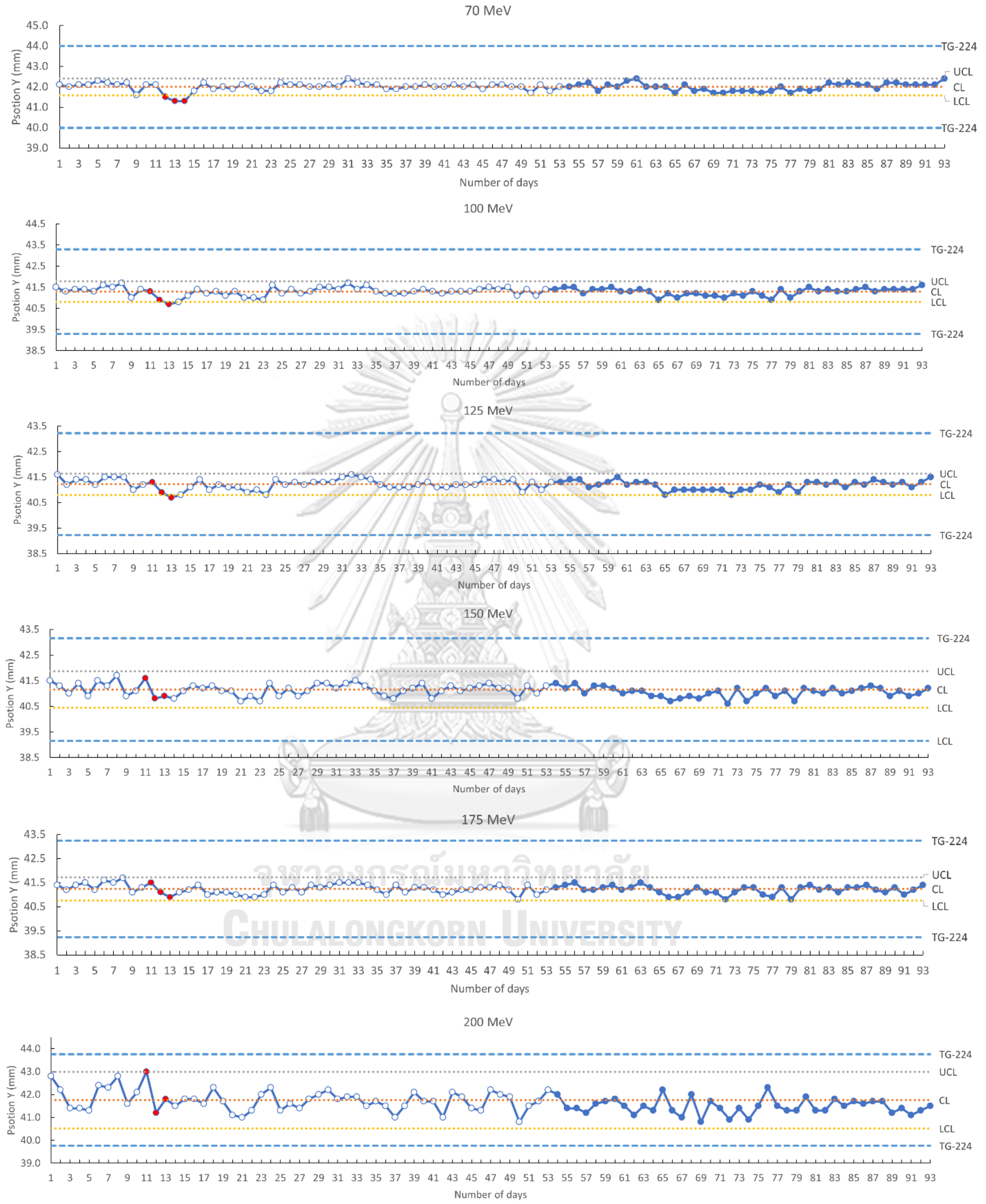

Figure 4.7 Control chart of spot position Y of 70 MeV, 100 MeV, 125 MeV, 150 MeV, 175 MeV, and 200 MeV.

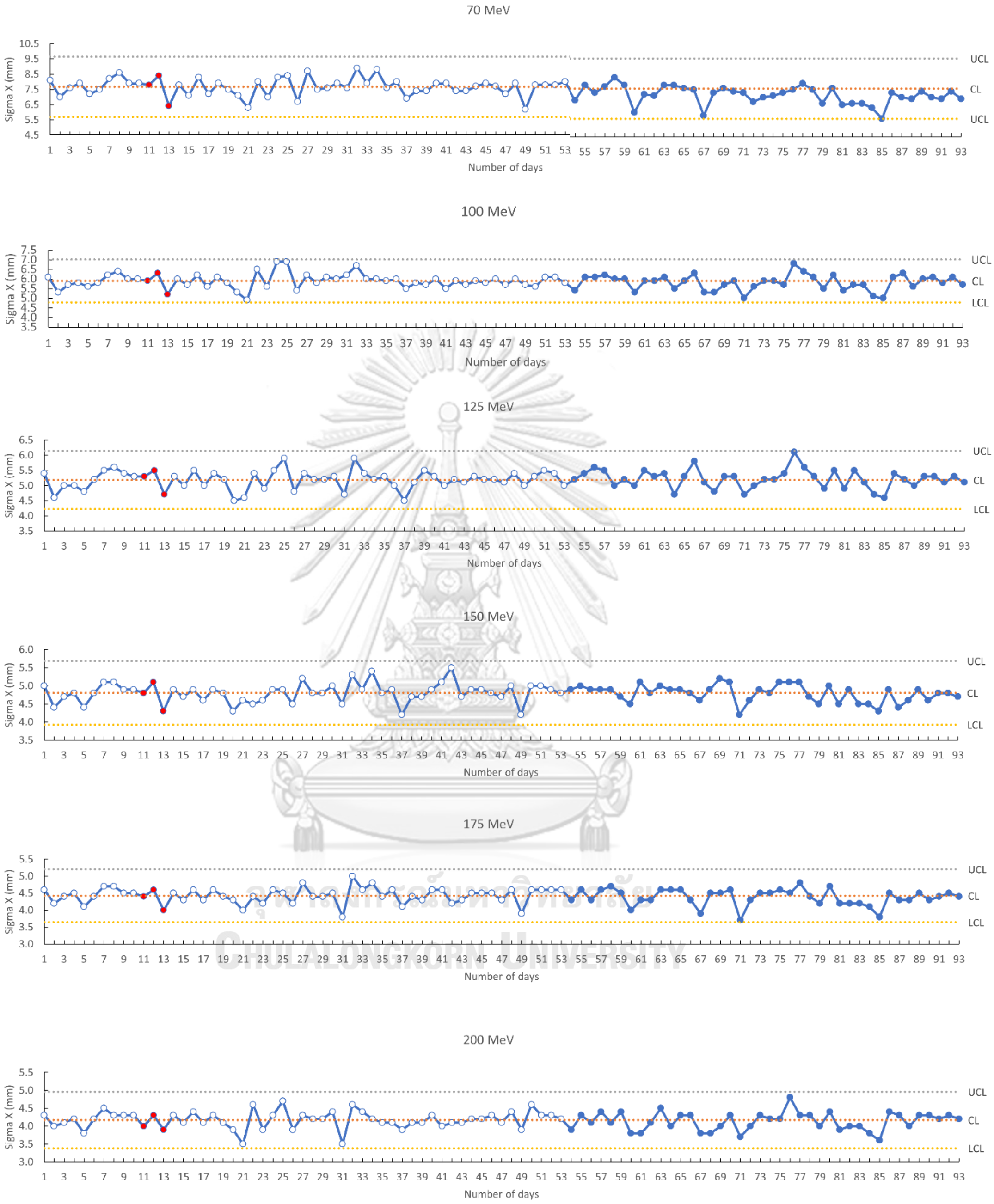

Figure 4.8 Control chart of spot sigma X of 70 MeV, 100 MeV, 125 MeV, 150 MeV, 175 MeV, and 200 MeV.

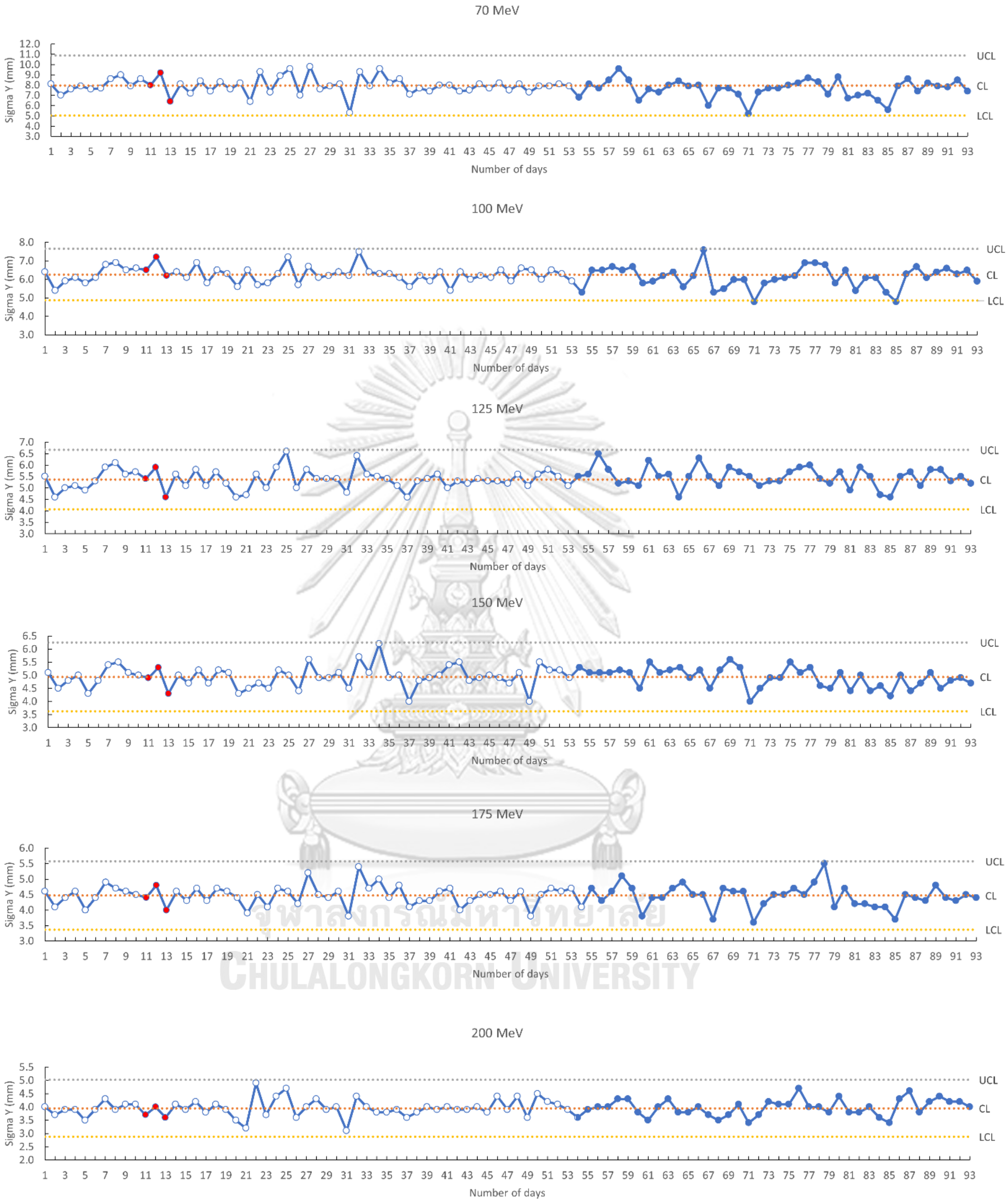

Figure 4.9 Control chart of spot sigma Y of 70 MeV, 100 MeV, 125 MeV, 150 MeV, 175 MeV, and 200 MeV.

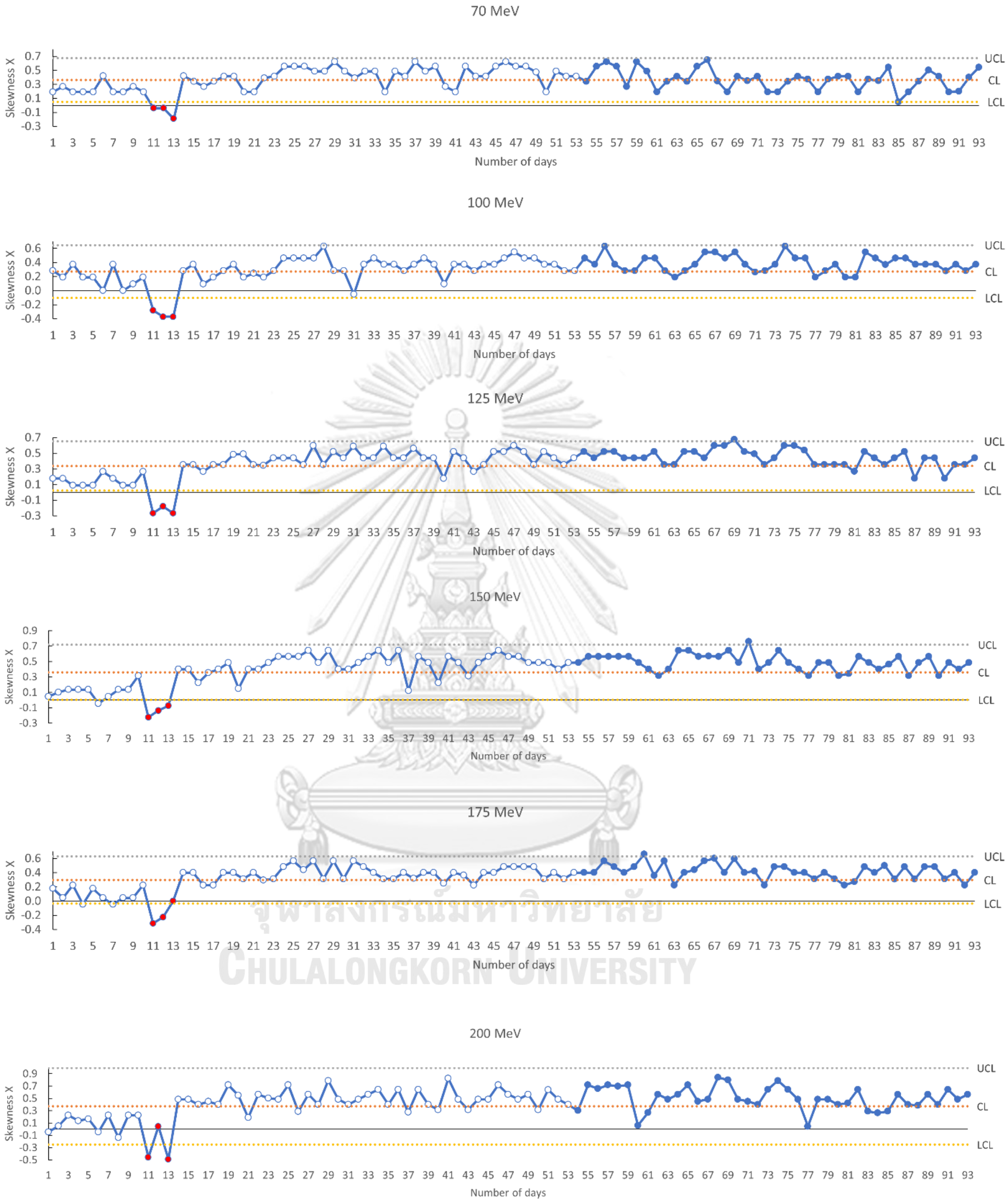

Figure 4.10 Control chart of spot skewness X of 70 MeV, 100 MeV, 125 MeV, 150 MeV, 175 MeV, and 200 MeV.

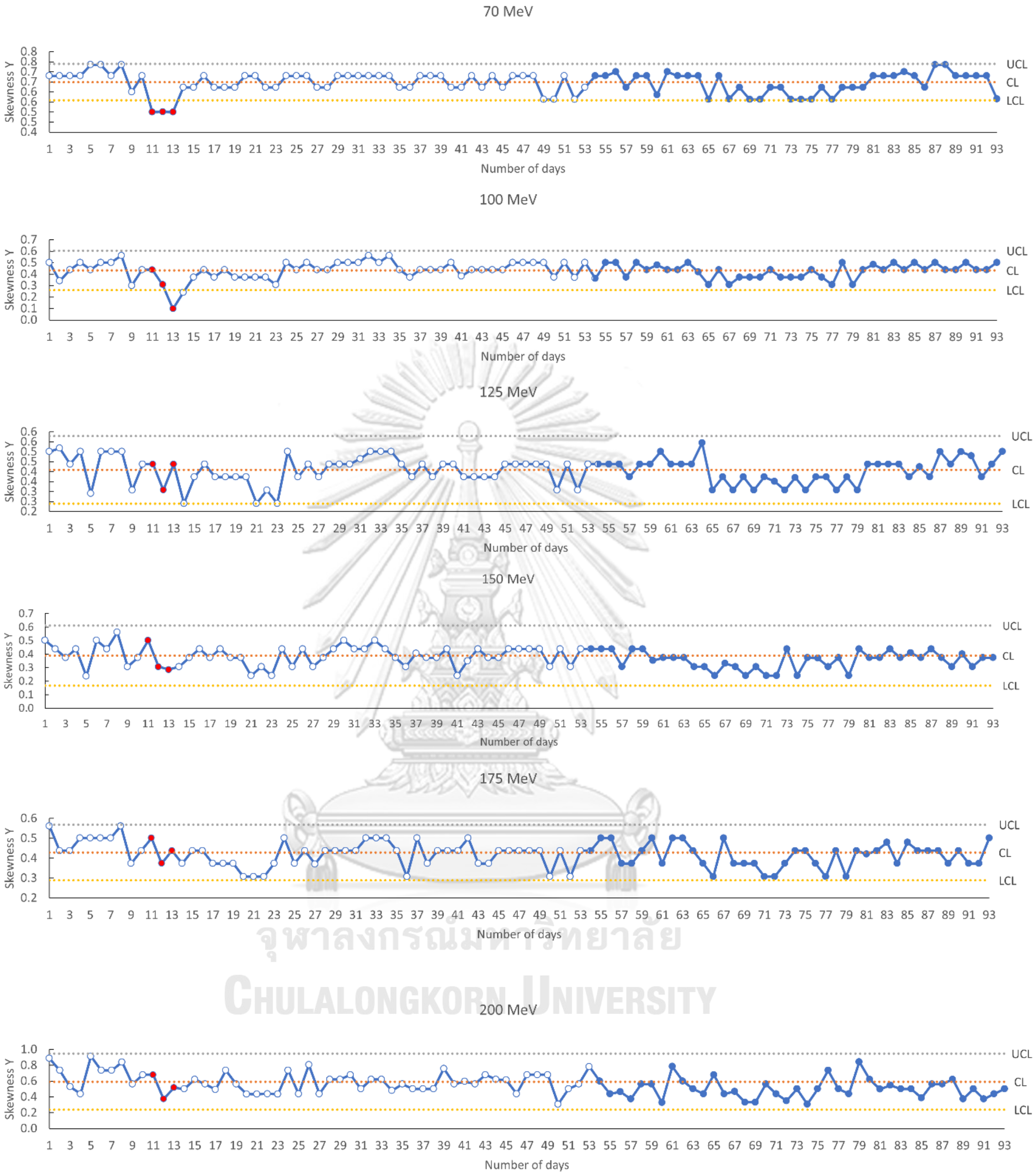

Figure 4.11 Control chart of spot skewness Y of 70 MeV, 100 MeV, 125 MeV, 150 MeV, 175 MeV, and 200 MeV.

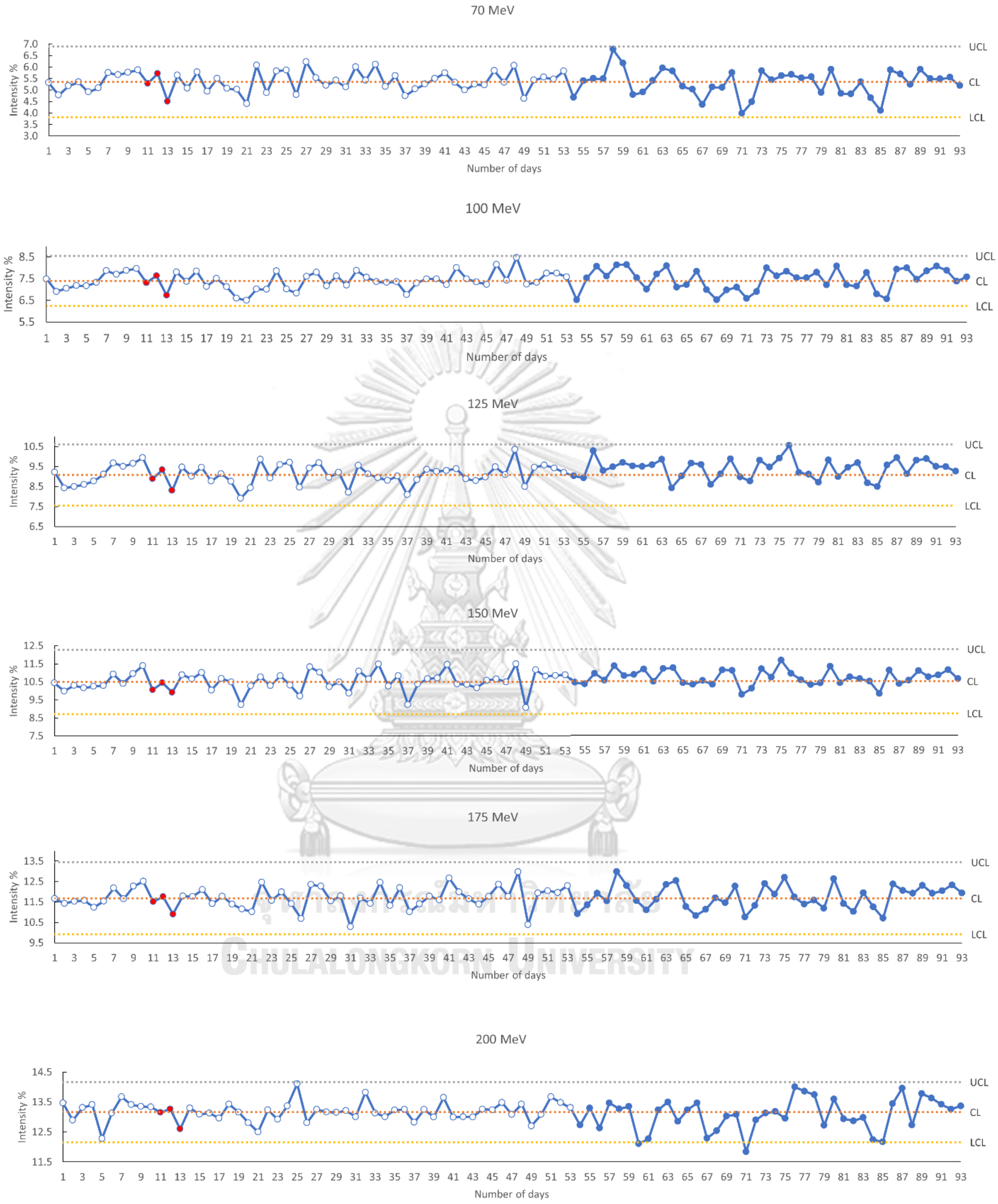

Figure 4.12 Control chart of spot intensity of 70 MeV, 100 MeV, 125 MeV, 150 MeV, 175 MeV, and 200 MeV.

4.3 Uniform field homogeneity

This task is the measurement of the flatness of the proton beam profile. The average value, upper control limit and lower control limit were calculated using 50 daily QA data. The average was 1.5 % and upper and lower limits were ± 0.7 %.

4.4 Coincidence

This task was the measurement of the x-ray/proton coincidence. The average value, upper control limit and lower control limit were calculated using 50 daily QA data. The average value was 0.2 mm in both X and Y directions. The upper and lower control limits were ± 0.4 mm and ± 0.2 mm in X and Y directions, respectively.

4.5 Dose output consistency

The proton dose output consistency was measured by The PPC05 detector inserted in the Sphinx Compact. The average value, upper control limit and lower control limit were calculated using 50 daily QA data. The average charge was 1.083 nC. The upper and lower control limits were 0.01 nC.

Control limits for both coincidence X and Y, uniform field homogeneity and dose output consistency are shown in table 4.3. The control charts of x-ray/proton coincidence, homogeneity, and dose output are shown in figures 4.13 – 4.15. As mentioned above in section 4.2 the red dots in control charts were the excluded data which not been used for calculating the baselines due to the data are in out of limit zone.

Table 4.5 Control limits for uniform field homogeneity, dose output consistency and proton/x-ray coincidence.

Parameters	Average	Control limits
Coincidence X	0.2 mm.	± 0.4 mm.
Coincidence Y	0.2 mm.	± 0.2 mm.
Homogeneity	1.5 %	± 0.7 %
Dose output	1.083 nC	± 0.010 nC

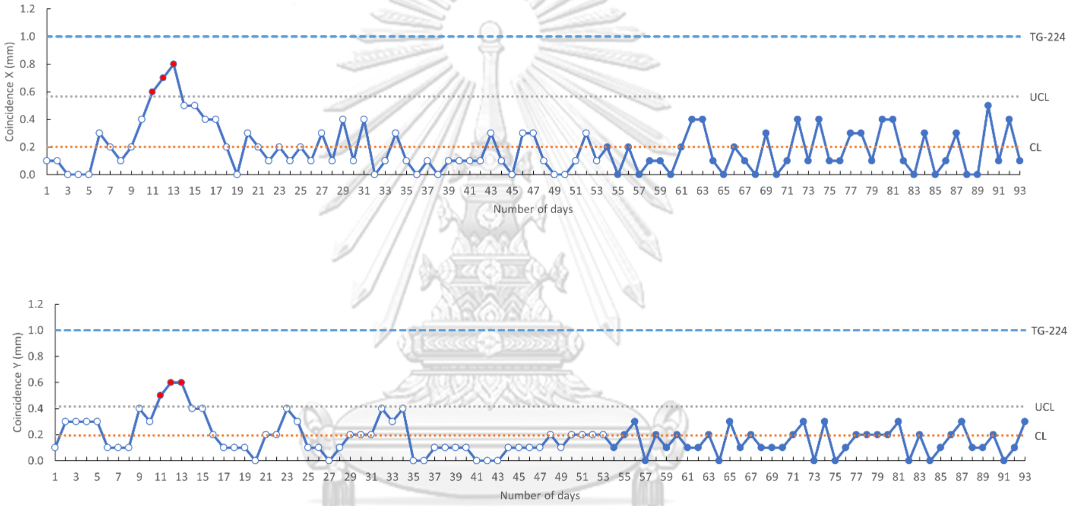

Figure 4.13 Control chart of x-ray/proton coincidence in X and Y direction.

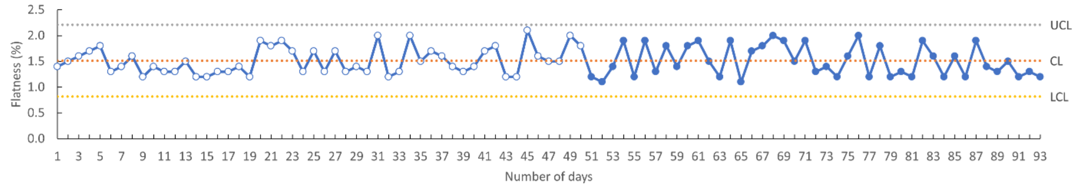

Figure 4.14 Control chart of uniform field homogeneity.

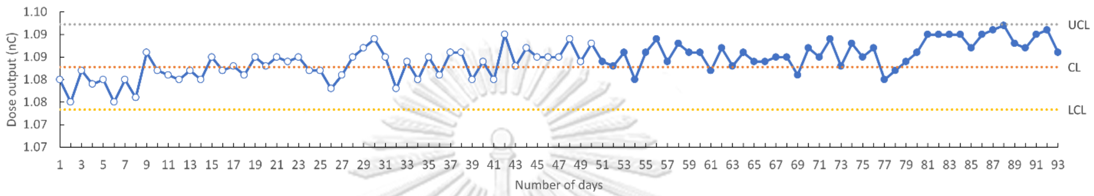

Figure 4.15 Control chart of dose output consistency.

CHAPTER 5
DISCUSSION AND CONCLUSION

5.1 Energy characteristics

Table 5.1 is the control limits from this study compared to other literature and TG-224. Compare to results from other published literature and Rena S. study(5) which used the Lynx scintillation detector. The results were comparable. The distal depth limits from this study and Rena S. are less than the limits set by Lambert J.(13), Bizzocchi N.(14) The Sphinx Compact detector can be used to perform daily QA tasks in proton pencil beam scanning energy characteristics. The highest limits of 0.5 mm were from 200 MeV in all energy characteristics tasks: distal depth, distal fall off, proximal depth, and peak width. For convenience limit setup, 0.5 mm is suggested for all energy-characteristic tasks.

Table 5.1 Control limits for energy characteristics compared to published literature and TG-224.

Parameters	Energy (MeV)	Control limits			
		This study (mm)	Rena S. (mm)	Published literature (mm)	TG-224 (mm)
Distal depth	100	± 0.1	± 0.3	± 1 (13), ± 2 (14)	± 1.0 mm
	150	± 0.3			
	200	± 0.5			
Distal fall off	100	± 0.2	± 0.3	NA	NA
	150	± 0.3			
	200	± 0.5			

Table 5.2 Control limits for energy characteristics compared to published literature and TG-224 (cont.).

Parameters	Energy (MeV)	Control limits			
		This study (mm)	Rena S. (mm)	Published literature (mm)	TG-224 (mm)
Proximal depth	100	± 0.4	± 0.0	NA	NA
	150	± 0.3	± 0.1		
	200	± 0.5			
Peak width	100	± 0.4	± 0.2	NA	NA
	150	± 0.4			
	200	± 0.5			

5.2 **Spot characteristics**

All the results in spot characteristics were comparable with other published literature (5, 13, 14), and the limits in spot position X and Y direction were comparable with those from Rena S. and less than the results from Lambert J., Bizzocchi N., and AAPM TG-224 (4), which were 2.0 mm, as shown in table 5.2. However, the spot sigma result was incompatible with the Rena S. study (5)Rena S. reported an increasing percentage difference with increasing proton energy, while the limits of spot sigma in this study decreased with increasing proton energy caused by the ROI dependence in the myQA software analysis process.

Table 5.3 Control limits for spot characteristics compared to published literature and TG-224.

Parameters	Energy (MeV)	Control limits			
		This study (mm)	Rena S.	Published literature	TG-224 (mm)
Spot position X	70	± 1.0	± 0.6 mm.	± 1 mm. (14), ± 1.5 mm. (13)	± 2.0
	100	± 0.7			
	125	± 0.8			
	150	± 0.8			
	175	± 0.7			
	200	± 1.2			
Spot position Y	70	± 0.5	± 0.4 mm.	± 1 mm. (14), ± 1.5 mm. (13)	± 2.0
	100	± 0.5			
	125	± 0.4			
	150	± 0.7			
	175	± 0.5			
	200	± 0.8			
Spot sigma X	70	± 2.0	NA	± 10 %(13), ± 15 %(14)	NA
	100	± 1.3	± 0.9 %		
	125	± 1.0	NA		
	150	± 0.9	± 1.7 %		
	175	± 0.8	± 1.9 %		
	200	± 0.8	± 2.1 %		
Spot sigma Y	70	± 2.9	NA	± 10 %(13), ± 15 %(14)	NA
	100	± 1.4	± 1.1 %		
	125	± 1.3	NA		
	150	± 1.3	± 2.0 %		
	175	± 1.1	± 2.7 %		
	200	± 1.1	± 3.6 %		

Table 5.4 Control limits for spot characteristics compared to published literature and TG-224 (cont.).

<table>
<tr><th rowspan="2">Parameters</th><th rowspan="2">Energy (MeV)</th><th colspan="4">Control limits</th></tr>
<tr><th>This study</th><th>Rena S.</th><th>Published literature</th><th>TG-224</th></tr>
<tr><td rowspan="6">Spot skewness X</td><td>70</td><td>± 0.380</td><td>NA</td><td rowspan="6">NA</td><td rowspan="6">NA</td></tr>
<tr><td>100</td><td>± 0.315</td><td>± 0.2</td></tr>
<tr><td>125</td><td>± 0.333</td><td>NA</td></tr>
<tr><td>150</td><td>± 0.357</td><td rowspan="3">± 0.3</td></tr>
<tr><td>175</td><td>± 0.334</td></tr>
<tr><td>200</td><td>± 0.621</td></tr>
<tr><td rowspan="6">Spot skewness Y</td><td>70</td><td>± 0.119</td><td>NA</td><td rowspan="6">NA</td><td rowspan="6">NA</td></tr>
<tr><td>100</td><td>± 0.191</td><td>± 0.2</td></tr>
<tr><td>125</td><td>± 0.175</td><td>NA</td></tr>
<tr><td>150</td><td>± 0.222</td><td>± 0.2</td></tr>
<tr><td>175</td><td>± 0.175</td><td rowspan="2">± 0.3</td></tr>
<tr><td>200</td><td>± 0.394</td></tr>
<tr><td rowspan="6">Intensity</td><td>70</td><td>± 1.5 %</td><td rowspan="6">NA</td><td rowspan="6">NA</td><td rowspan="6">NA</td></tr>
<tr><td>100</td><td>± 1.4 %</td></tr>
<tr><td>125</td><td>± 1.5 %</td></tr>
<tr><td>150</td><td>± 1.8 %</td></tr>
<tr><td>175</td><td>± 1.8 %</td></tr>
<tr><td>200</td><td>± 1.0 %</td></tr>
</table>

The decreasing trend of result in spot sigma was caused by the ROI dependence in the myQA analysis process, which is related to the % intensity in each spot. The parameter intensity was relative to the 200 MeV 8 MU/spot at the top left region of the QA plan as shown in Figure 5.1

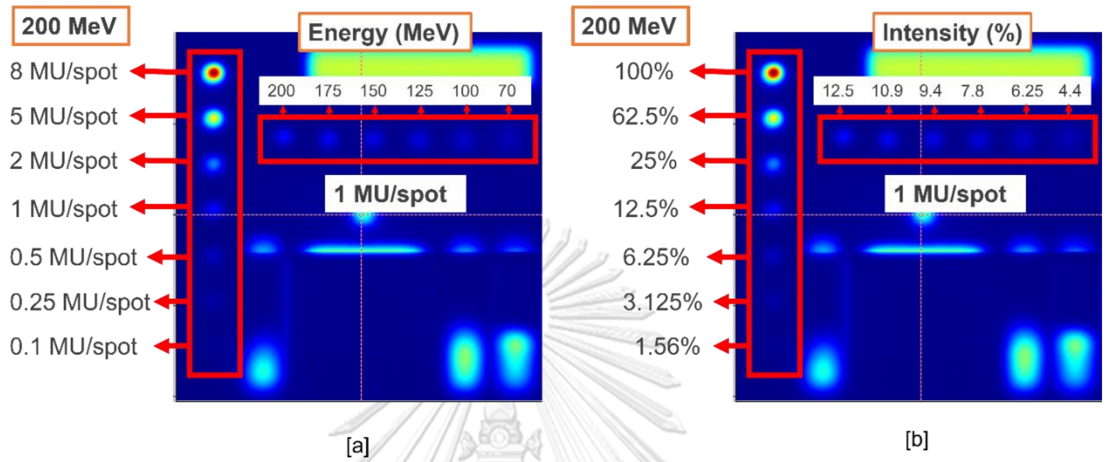

Figure 5.1 Comparison of spot energy and % intensity.
(a) MU in each spot, (b) % intensity in each spot

Spot characteristics region in myQA plan was created to give all spots 1 MU/spot in different energy. Thus, the intensity related to 200 MeV, 8 MU/spot of each energy in this region were 12.5 %, 10.9 %, 9.4 %, 7.8 %, 6.25 % and 4.4 % for 200 MeV, 175 MeV, 150 MeV, 125 MeV, 100 MeV, and 70 MeV, respectively. In the performing process, it is a big challenge to keep all the spots located at the exact center of the ROI. Therefore, the results from 70 MeV, 4.4 % intensity, were the most affected by the ROI dependence causing the results of the highest variation. This ROI dependence related to % intensity was the reason that the limits from spot sigma were decreasing with increasing proton energy.

For the spot position, the highest limit of ± 1.2 mm was found at 200 MeV in the X direction which is still less than the AAPM TG-224 recommendation. For convenient limits setup, ± 1.2 mm are suggested for all energies in spot position. For spot sigma, the highest limit was ± 2.9 mm, the lowest was ± 0.8 mm, and the difference between the highest and lowest was 2.1 mm, which seems to be a high number compared to the average value of each energy. The separately control limits setup in each energy are suggested for spot sigma.

5.3 X-ray/proton coincidence

The results from x-ray/proton coincidence were comparable with Rena S. and Lambert J. and less than the limits recommended by TG-224 which were ± 1.0 mm as shown in table 5.3. The results showed a relation between coincidence, spot position and spot skewness on account of data in date number 11, 12, and 13 in coincidence in X direction showing an out-of-limit value which might be caused by setup error while performing the daily QA tests. We excluded data from these 3 days from calculating the baselines and control limits to reduce the systematic error on control chart limits.

Figure 5.2 – 5.4 show the out-of-limit trend that is also found in date number 11, 12, and 13 in spot position and spot skewness as well. Performing the daily QA tasks in x-ray/proton coincidence as low as possible was suggested.

Table 5.5 Control limits for x-ray/proton coincidence compared to other published literature and TG-224.

<table>
<tr><th></th><th>Limits (mm)</th><th>Rena S. (mm)</th><th>Lambert J. (mm)</th><th>TG-224 (mm)</th></tr>
<tr><td>Coincidence X</td><td>± 0.4</td><td>± 0.7</td><td rowspan="2">± 1.5</td><td rowspan="2">± 1.0</td></tr>
<tr><td>Coincidence Y</td><td>± 0.2</td><td>± 0.5</td></tr>
</table>

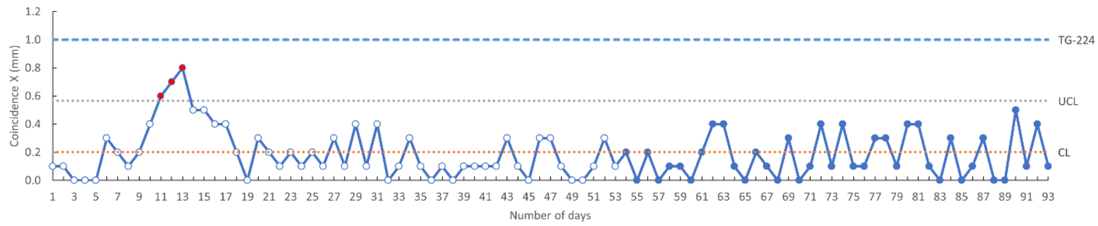

Figure 5.2 Control chart of x-ray/proton coincidence in X direction.

out of limit trend in date number 11, 12, and 13

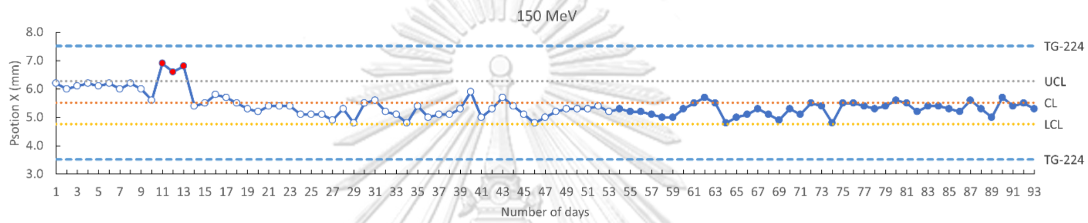

Figure 5.3 Control chart of spot position X of 150 MeV.

out of limits trend in date number 11, 12, and 13

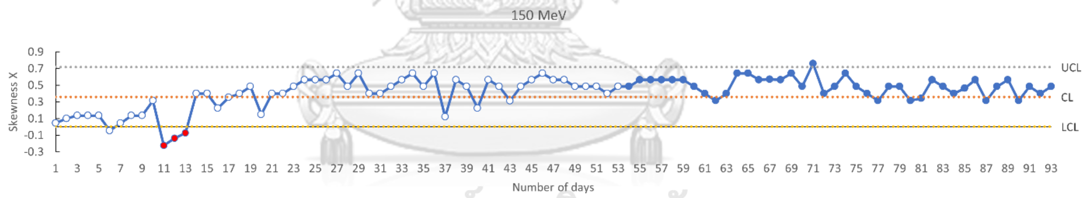

Figure 5.4 Control chart of spot skewness X of 150 MeV.

out of limits trend in date number 11, 12, and 13

5.4 myQA control limits setup

All the results were set to be the baselines in myQA analysis which need 3 values to setup; expected value, warning value, and failed value. There are 2 groups to setup myQA. First is tasks that available in TG-224 include distal depth, spot position and x-ray/proton coincidence, the value from CL was used to setup expected value, the UCL and LCL were used to set up warning value and failed was the limits recommended by TG-224. Second is tasks that not available in TG-224 include distal falloff, proximal depth, peak width, spot sigma, spot skewness, spot intensity, uniform field homogeneity, and dose output consistency. The values from CLs were used to setup the expected value as well, for warning value ± $2X_{indi}$ were used, and the failed uses UCL and LCL to setup. Table 5.4 – 5.6 show the setup value for myQA software.

Table 5.6 myQA setup for energy characteristics.

Energy (MeV)	Parameters	Expected (mm.)	Warning (mm.)	Action (mm.)
100	Distal depth	75.7	± 0.1	± 1.0
	Distal fall off	3.0	± 0.1	± 0.2
	Proximal depth	69.4	± 0.2	± 0.4
	Peak width	6.3	± 0.3	± 0.4
150	Distal depth	155.9	± 0.3	± 1.0
	Distal fall off	5.0	± 0.2	± 0.3
	Proximal depth	147.5	± 0.2	± 0.3
	Peak width	8.4	± 0.3	± 0.4
200	Distal depth	257.0	± 0.5	± 1.0
	Distal fall off	6.0	± 0.3	± 0.5
	Proximal depth	251.1	± 0.3	± 0.5
	Peak width	5.9	± 0.3	± 0.5

Table 5.7 myQA setup for spot characteristics.

Energy (MeV)	Parameters	Expected	Warning	Action
70	Position X	80.7 mm.	± 1.0 mm.	± 2.0 mm.
	Position Y	42.0 mm.	± 0.5 mm.	± 2.0 mm.
	Sigma X	7.7 mm.	± 1.3 mm.	± 2.0 mm.
	Sigma Y	8.0 mm.	± 1.9 mm.	± 2.9 mm.
	Skewness X	0.366	± 0.254	± 0.380
	Skewness Y	0.653	± 0.079	± 0.119
	Intensity	5.4 %	± 1.0 %	± 1.5 %
100	Position X	55.6 mm.	± 0.7 mm.	± 2.0 mm.
	Position Y	41.3 mm.	± 0.5 mm.	± 2.0 mm.
	Sigma X	5.9 mm.	± 0.9 mm.	± 1.3 mm.
	Sigma Y	6.3 mm.	± 0.9 mm.	± 1.4 mm.
	Skewness X	0.223	± 0.210	± 0.315
	Skewness Y	0.428	± 0.128	± 0.191
	Intensity	7.4 %	± 0.9 %	± 1.4 %
125	Position X	30.8 mm.	± 0.8 mm.	± 2.0 mm.
	Position Y	41.2 mm.	± 0.4 mm.	± 2.0 mm.
	Sigma X	5.2 mm.	± 0.6 mm.	± 1.0 mm.
	Sigma Y	5.4 mm.	± 0.9 mm.	± 1.3 mm.
	Skewness X	0.324	± 0.222	± 0.333
	Skewness Y	0.408	± 0.177	± 0.175
	Intensity	9.7 %	± 1.0 %	± 1.5 %

Table 5.8 myQA setup for spot characteristics (cont.).

Energy (MeV)	Parameters	Expected	Warning	Action
150	Position X	5.5 mm.	± 0.8 mm.	± 2.0 mm.
	Position Y	41.2 mm.	± 0.7 mm.	± 2.0 mm.
	Sigma X	4.8 mm.	± 0.6 mm.	± 0.9 mm.
	Sigma Y	4.9 mm.	± 0.9 mm.	± 1.3 mm.
	Skewness X	0.361	± 0.238	± 0.357
	Skewness Y	0.389	± 0.148	± 0.222
	Intensity	10.5 %	± 1.2 %	± 1.8 %
175	Position X	-19.2 mm.	± 0.7 mm.	± 2.0 mm.
	Position Y	41.2 mm.	± 0.5 mm.	± 2.0 mm.
	Sigma X	4.4 mm.	± 0.5 mm.	± 0.8 mm.
	Sigma Y	4.5 mm.	± 0.7 mm.	± 1.1 mm.
	Skewness X	0.286	± 0.223	± 0.334
	Skewness Y	0.414	± 0.116	± 0.175
	Intensity	11.7 %	± 1.2 %	± 1.8 %
200	Position X	-44.5 mm.	± 1.2 mm.	± 2.0 mm.
	Position Y	41.8 mm.	± 0.8 mm.	± 2.0 mm.
	Sigma X	4.2 mm.	± 0.5 mm.	± 0.8 mm.
	Sigma Y	4.0 mm.	± 0.7 mm.	± 1.1 mm.
	Skewness X	0.372	± 0.414	± 0.621
	Skewness Y	0.592	± 0.263	± 0.394
	Intensity	13.2 %	± 0.7 %	± 1.0 %

Table 5.9 myQA setup for x-ray/proton coincidence, homogeneity, and dose output consistency.

X-ray/proton coincidence			
Parameter	**Expected**	**Warning**	**Action**
Position X	5.5 mm.	± 0.8 mm.	± 2.0 mm.
Position Y	41.2 mm.	± 0.7 mm.	± 2.0 mm.
Uniform field homogeneity			
Parameter	**Expected**	**Warning**	**Action**
Flatness	1.5 %	± 0.5 %	± 0.7 %
Dose output consistency			
Parameter	**Expected**	**Warning**	**Action**
Output	1.083 nC	± 0.007 nC	± 0.01 nC

5.5 Conclusion

The control charts obtained by Sphinx Compact can be applied to set the baselines of daily QA data for proton pencil beam scanning at Her Royal Highness Princess Maha Chakri Sirindhorn Proton Therapy Center, KCMH.

REFERENCES

1. Sisterson J. Ion beam therapy in 2004. Nuclear Instruments and Methods in Physics Research Section B: Beam Interactions with Materials and Atoms. 2005;241(1-4):713-6.

2. Marchand B, Prieels D, Bauvir B. IBA PROTON PENCIL BEAM SCANNING AN INNOVATIVE SOLUTION. 2000.

3. Goughenour A. Modern pencil beam scanning (PBS) where we are and where we are going. 2017.

4. Arjomandy B, Taylor P, Ainsley C, Safai S, Sahoo N, Pankuch M, et al. AAPM task group 224: Comprehensive proton therapy machine quality assurance. Med Phys. 2019;46(8):e678-e705.

5. Rana S, Bennouna J, Samuel EJJ, Gutierrez AN. Development and long-term stability of a comprehensive daily QA program for a modern pencil beam scanning (PBS) proton therapy delivery system. J Appl Clin Med Phys. 2019;20(4):29-44.

6. Su Z, Hsi W, Forthomme J, Rossomme S. Evaluations of a flat-panel based compact daily quality assurance device for proton pencil beam scanning (PBS) system. Phys Med. 2020;80:243-50.

7. Newhauser WD, Zhang R. The physics of proton therapy. Phys Med Biol. 2015;60(8):R155-209.

8. Basile E, Carloni A, Castelluccio DM, Cisbani E, Colilli S, Angelis GD, et al. An online proton beam monitor for cancer therapy based on ionization chambers with micro pattern readout. Journal of Instrumentation. 2012;7(03):C03020-C.

9. Kotter E, Langer M. Digital radiography with large-area flat-panel detectors. Eur Radiol. 2002;12(10):2562-70.

10. F.Knoll G. Ionization chambers. Radiation Detection and Measurement. 1999.

11. Zhao L, Newton J, Oldham M, Das IJ, Cheng CW, Adamovics J. Feasibility of using PRESAGE(R) for relative 3D dosimetry of small proton fields. Phys Med Biol. 2012;57(22):N431-43.

12. Gustavsson H, Back SA, Medin J, Grusell E, Olsson LE. Linear energy transfer

dependence of a normoxic polymer gel dosimeter investigated using proton beam absorbed dose measurements. Phys Med Biol. 2004;49(17):3847-55.

13. Lambert J, Baumer C, Koska B, Ding X. Daily QA in proton therapy using a single commercially available detector. J Appl Clin Med Phys. 2014;15(6):5005.

14. Bizzocchi N, Fracchiolla F, Schwarz M, Algranati C. A fast and reliable method for daily quality assurance in spot scanning proton therapy with a compact and inexpensive phantom. Med Dosim. 2017;42(3):238-46.

VITA

NAME	Tanapat Tiajaroen
DATE OF BIRTH	25 June 1996
PLACE OF BIRTH	Saraburi
INSTITUTIONS ATTENDED	B.Sc. in Science (Radiological Technology), Chulalongkorn University, Thailand
HOME ADDRESS	62/6 moo 7, Kumphram, Wang Muang, Saraburi, 18220
PUBLICATION	“27th Annual Thai Society of Radiological Technologists Conference, Bangkok, Thailand. April 24-26, 2019. Gamma-H2AX biodosimetry for evaluation of DNA damage in blood leucocyte after external ex-vivo irradiation. T. Tiajaroen, Y. Buranasakulsatid, T. Tippayamontri. (Poster presentation).